Helsinki University of Technology
Laboratory of Forest Products Chemistry, Reports Series A25
Espoo 2006

SURFACE INTERACTIONS IN TMP PROCESS WATERS

Tekla Tammelin

TEKNILLINEN KORKEAKOULU
TEKNISKA HÖGSKOLAN
HELSINKI UNIVERSITY OF TECHNOLOGY
TECHNISCHE UNIVERSITÄT HELSINKI
UNIVERSITE DE TECHNOLOGIE D'HELSINKI

Helsinki University of Technology
Laboratory of Forest Products Chemistry, Reports Series A25
Espoo 2006

SURFACE INTERACTIONS IN TMP PROCESS WATERS

Tekla Tammelin

Dissertation for the degree of Doctor of Science in Technology to be presented with due permission of the Department of Forest Products Technology for public examination and debate in PUU 2 Auditorium at Helsinki University of Technology (Espoo, Finland) on the 1st of December, 2006, at 12 noon.

Helsinki University of Technology
Department of Forest Products Technology
Laboratory of Forest Products Chemistry

Teknillinen korkeakoulu
Puunjalostustekniikan osasto
Puunjalostuksen kemian laboratorio

Distribution:
Helsinki University of Technology
Laboratory of Forest Products Chemistry
P.O. Box 6300
FI-02015 TKK, Finland
URL: http://www.tkk.fi/Units/Forestpc/
Tel. +358 9 4511
Fax +358 9 451 4259

ISBN-13 978-951-22-8482-5
ISBN-10 951-22-8482-0
ISBN-13 978-951-22-8483-2 (PDF)
ISBN-10 951-22-8483-9 (PDF)
ISSN 1457-1382
ISSN 1795-2409 (E)
URL: http://lib.tkk.fi/Diss/2006/isbn9512284839/

Picaset Oy
Helsinki 2006

HELSINKI UNIVERSITY OF TECHNOLOGY P. O. BOX 1000, FI-02015 TKK http://www.tkk.fi	ABSTRACT OF DOCTORAL DISSERTATION

Author Tekla Tammelin

Name of the dissertation

Surface interactions in TMP process waters

Date of manuscript August 28, 2006	Date of the dissertation December 1, 2006
☐ Monograph	☒ Article dissertation (summary + original articles)

Department	Forest Products Technology
Laboratory	Forest Products Chemistry
Field of research	Chemistry of Forest Products Technology
Opponent(s)	Professor Orlando Rojas
Supervisor	Professor Janne Laine
(Instructor)	Docent Monika Österberg and Professor (emeritus) Per Stenius

Abstract

The overall goal of the thesis was to better understand on a molecular level different interactions present in the wet-end of the paper machine that uses thermomechanical (TMP) pulp. The work is divided into three parts:

1) Introduction of the QCM-D technique to papermaking applications (polyelectrolyte adsorption studies)
2) Development of model surfaces for cellulose, lignin and wood extractives for adsorption studies
3) Adsorption studies of dissolved hemicelluloses and colloidal wood extractives on the model surfaces

The work was started by studying the adsorption of cationic starch onto the oppositely charged silica surface with the quartz crystal microbalance with dissipation (QCM-D). The aim of these preliminary adsorption studies was to better understand the electrostatic interactions between polyelectrolyte and surface, the factors which have influence on adsorption and the structure and physical properties of the adsorbed layer. The results were in accordance with the well-known theories of the polyelectrolyte adsorption

In order to investigate the surface interactions in the TMP process waters, model surfaces for cellulose, lignin and wood extractives were prepared. In this way the interactions between the components originating from the pulp (dissolved and colloidal substances) and the fibrous material could be systematically studied. Raw materials were chosen so that they represent the main components present in a papermaking stock containing TMP. Atomic force microscopy (AFM) and X-ray photoelectron spectroscopy (XPS) were used to investigate the morphology and chemistry of the model surfaces.

Finally, the adsorption of dissolved hemicelluloses and colloidal extractives on different fiber components were studied with the QCM-D. The aim was to clarify how colloidal resin and dissolved substances interact and how these interactions depend on e.g. peroxide bleaching of the TMP and ionic strength. It was found that dissolved hemicelluloses adsorb at the largest on cellulose. They also adsorbed on extractives but there was no significant affinity towards lignin. Adsorption increased with increasing ionic strength on cellulose and on extractives. Colloidal extractives preferentially adsorbed on cellulose when only electrostatically stabilized. The dissolved hemicelluloses created a steric hindrance against colloidal adsorption on all surfaces, but the effect was most pronounced on cellulose. The adsorption of colloids increased with increasing ionic strength for almost all systems. On the basis of the fundamental surface studies, some practical observations achieved from the experiments with the fine material could be clarified.

Keywords Adsorption, colloidal extractives, dissolved hemicelluloses, model surfaces, AFM, TMP, QCM-D, XPS

ISBN (printed) 951-22-8482-0	ISSN (printed) 1457-1382
ISBN (pdf) 951-22-8483-9	ISSN (pdf) 1795-2409
ISBN (others)	Number of pages 82

Publisher Helsinki University of Technology, Laboratory of Forest Products Chemistry

Print distribution Helsinki University of Technology, Laboratory of Forest Products Chemistry

☒ The dissertation can be read at http://lib.tkk.fi/Diss/2006/isbn9512284839

TEKNILLINEN KORKEAKOULU PL 1000, 02015 TKK http://www.tkk.fi	VÄITÖSKIRJAN TIIVISTELMÄ
Tekijä Tekla Tammelin	
Väitöskirjan nimi Pintavuorovaikutukset kuumahierreprosessin (TMP) vesissä	
Käsikirjoituksen jättämispäivämäärä 22.8.2006	Väitöstilaisuuden ajankohta 1.12.2006
☐ Monografia	☒ Yhdistelmäväitöskirja (yhteenveto + erillisartikkelit)
Osasto Puunjalostustekniikka Laboratorio Puunjalostuksen kemian laboratorio Tutkimusala Puunjalostuksen kemia Vastaväittäjä(t) Professori Orlando Rojas Työn valvoja Professori Janne Laine (Työn ohjaaja) Dosentti Monika Österberg ja professori (emeritus) Per Stenius	

Tiivistelmä

Työn tarkoituksena on ymmärtää paremmin sellaisen paperikoneen märänpään pinta- ja kolloidikemiaa, mikä käyttää raaka-aineenaan kuumahierrettä. Työ on jaettu kolmeen osaan:

1) QCM-D tekniikan käyttöönotto paperinvalmistussovelluksessa
2) Kuitumateriaalin (selluloosa, ligniini ja pihla) mallipintojen valmistus ja karakterisointi
3) Kuumahierteen pihka-aineiden, liuenneiden hemiselluloosien ja kuidun pääkomponenttien välisten vuorovaikutuksien tutkiminen

Työ aloitettiin tutkimalla kationisen tärkkelyksen sitoutumista vastakkaismerkkiselle piipinnalle kvartsikidemikrovaa’alla (QCM-D).Tämä adsorptiotutkimus oli perustutkimusta, jonka tarkoituksena oli ymmärtää paremmin polyelektrolyytin ja pinnan sähköstaattisia vuorovaikutuksia, adsorptioon vaikuttavia tekijöitä, adsorboituneen kerroksen rakennetta ja sen fysikaalisia ominaisuuksia. Tulokset noudattivat hyvin tunnettuja polyelektrolyytiadsorptioteorioita.

Työtä jatkettiin kehittämällä mallipintoja, joiden tarkoituksena on mallintaa kuidun pääkomponentteja (selluloosa, ligniini ja pihka) erikseen. Raaka-aineet valittiin siten, että ne edustavat kuumahierreprosesissa läsnä olevia komponentteja. Näitä pintoja käytettiin QCM-D laitteella tehtävissä adsorptiomittauksissa. Tällä tavalla saatiin spesifistä tietoa pihka-aineiden ja hiilihydraattien käytöksestä ja sitoutumisesta mekaanisesta massasta paperia valmistavan koneen märässä päässä ja kuinka esim. peroksidi valkaisu ja ionivahvuus vaikuttavat sitoutumiseen. Mallipintojen ominaisuuksia karakterisoitiin atomivoimamikroskoopilla (AFM) ja röntgenfotoelektronisella spektroskoopilla (XPS).

Lopuksi liuenneiden hemiselluloosien ja kolloidaalisen pihkan adsorptiota kuidun pääkomponenteille tutkittiin QCM-D laitteella. Liuenneet hemiselluloosat adsorboituivat eniten selluloosalle. Ne adsorboituivat myös pihkapinnoille, mutta ligniinille adsorptio oli vähäistä. Adsorption määrä kasvoi ionivahvuuden kasvaessa selluloosalle ja pihkalle. Sähköstaattisesti stabiilit pihkakolloidit adsorboituivat eniten selluloosalle. Liuenneet hiilihydraatit muodostivat steerisen esteen ja kolloidien adsorptio pintoihin estyi. Havaittu vaikutus oli voimakkain selluloosapintojen tapauksessa. Näiden tulosten avulla pystyttiin selventämään havaintoja, joita saatiin tehdessä käytännön kokeita hienoaineksella.

Asiasanat Adsorptio, uuteainekolloidi, liuenneet hemiselluloosat, mallipinta, AFM, TMP, QCM-D, XPS	
ISBN (painettu) 951-22-8482-0	ISSN (painettu) 1457-1382
ISBN (pdf) 951-22-8483-9	ISSN (pdf) 1795-2409
ISBN (muut)	Sivumäärä 82
Julkaisija Teknillinen korkeakoulu, Puunjalostuksen kemian laboratorio	
Painetun väitöskirjan jakelu Teknillinen korkeakoulu, Puunjalostuksen kemian laboratorio	
☒ Luettavissa verkossa osoitteessa http://lib.tkk.fi/Diss/2006/isbn9512284839	

Preface

This study was carried out at the Laboratory of Forest Products Chemistry, Helsinki University of Technology, between the years 2004 and 2006.

The industrial financier, Kemira Oyj, is gratefully acknowledged for its contribution to this work. In addition, I wish to express my gratitude to Nordisk Forskerutdanningsakademi (NorFA), the Foundation of Magnus Ehrnrooth and the Foundation of Technology (TES) for granting funds for this research.

I am indebted to Professor Janne Laine and Professor (emeritus) Per Stenius for their excellent guidance in the challenging world of surface and colloid chemistry. I vastly appreciate the way you created an inspiring atmosphere for conducting research. Docent Monika Österberg is acknowledged with gratitude for sharing her extensive knowledge in physical chemistry and in AFM result interpretation as well as for supervising my scientific writing. Dr. Leena-Sisko Johansson is gratefully acknowledged for the valuable comments regarding the analysis of the XPS results. My co-authors and collegues, Ingvild A. Johnsen, M.Sc. at PFI, Norway and Terhi Saarinen, Lic. Sc. (Tech) are warmly thanked for their collaboration. It has been an honor to work in a research group with such a valuable scientific insight.

The personnel at the Laboratory of Forest Products Chemistry are thanked for the great and creative working atmosphere. In particular, I thank Ritva Kivelä, Marja Kärkkäinen and Aila Rahkola for accurate and high-quality laboratory work. Without you, the amount of reliable results would have been negligible. Timo Pääkkönen and Anu Anttila are also thanked for their skilful laboratory assistance and friendship. Our librarian, Kati Mäenpää is thanked for her swift help with the literature acquisitions. I am also very grateful to Kristiina Holm and Riitta Hynynen for keeping numerous practical issues under control. Juha Lindfors is thanked for patiently solving the problems with figures. My special thanks go to the joyful “coffee group” which has introduced terms such as “bloody unstable colloids” to the public, to name but one of many terms.

Laboratory of Wood and Paper Chemistry, Åbo Akademi University is acknowledged for donating the galactoglucomannan and pectin samples.

I wish to thank Karoliina Iivonen for the design and drawing of the cover of this book and Erja Holmström for the linguistic revision of the first version of the thesis.

All my precious relatives, numerous friends at horse stables and in motor cycle circles as well as former fellow students are thanked for their continuous support.

Finally, I warmly thank Pelle and my mother for their love and encouragement throughout these years.

Espoo, October 31st, 2006

Tekla Tammelin

To Pelle

TABLE OF CONTENTS

1 LIST OF PUBLICATIONS

This thesis is mainly based on the results presented in five publications which are referred as Roman numerals in the text. Some additional published and unpublished data is also related to the work.

Paper I
Tammelin, T., Merta, J., Johansson, L.-S. and Stenius, P. (2004) Viscoelastic properties of cationic starch adsorbed on quartz studied by QCM-D. *Langmuir* 20: 10900-10909.

Paper II
Tammelin, T., Saarinen, T., Österberg, M. and Laine J. (2006) Preparation of Langmuir-Blodgett –cellulose surfaces by using horizontal dipping procedure. Application for polyelectrolyte adsorption studies performed with QCM-D. *Cellulose*, 13: 519-535.

Paper III
Tammelin, T., Österberg, M., Johansson, L.-S. and Laine, J. (2006) Preparation of lignin and extractive model surfaces by using spincoating technique. Application for QCM-D crystals. *Nordic Pulp and Paper Research Journal* 21:444-450.

Paper IV
Tammelin, T., Johnsen, I. A., Österberg, M. Stenius, P. and Laine, J. (2006) Adsorption of colloidal extractives and dissolved hemicelluloses on thermomechanical pulp fiber components studied by QCM-D. *Nordic Pulp and Paper Research Journal*, accepted.

Paper V
Johnsen, I. A., Stenius, P., Tammelin T., Österberg, M. and Laine, J. (2006) The influence of dissolved substances on resin adsorption to TMP fine material. *Nordic Pulp and Paper Research Journal*, accepted.

AUTHOR'S CONTRIBUTION

I-IV Tekla Tammelin was responsible for the experimental design, performed the model surface preparations, QCM-D measurements and partly AFM measurements, analyzed the results, performed the modelings and wrote the manuscript.

V Tekla Tammelin defined the research plan with the co-authors, performed the QCM-D experiments and analyzed the experimental work and wrote the manuscript with a co-author.

Other related publications:

Paper VI
Kontturi, E., Tammelin T. and Österberg, M. (2006) Cellulose – model films and the fundamental approach. Review article. *Chemical Society Reviews*, DOI:10.1039/B601872F.

Paper VII
Tammelin, T., Österberg, M., Saarinen T., Johansson, L.-S. and Laine J. Development of model surfaces for different pulp fibre components. The 13th ISWFPC Conference Proceedings, Vol 2, 16-19 May, Auckland, New Zealand, 2005, 59-66

Paper VIII
Merta, J., Tammelin, T. and Stenius, P. (2004) Adsorption of complexes formed by cationic starch and anionic surfactans on quartz studied by QCM-D. *Colloids and Surfaces A: Physicochemical and Engineering Aspects* 250: 103-114.

Paper IX
Mosbye, J., Tammelin T., Saarinen T. and Laine J. (2004) The ability of PEO to remove model colloidal extractives from solutions with different types of fines. *Nordic Pulp and Paper Research Journal* 19: 59-66.

2 INTRODUCTION AND OUTLINE OF THE STUDY

This thesis presents fundamental surface chemistry studies with the aim to better explain on a molecular level the interactions present in the wet end of the paper machine when dissolved and colloidal substances are present together with fibrous material.

This work was a part of an industrial project carried out in cooperation with Kemira Oyj and Laboratory of Paper and Printing Technology. A part of the research work was conducted in cooperation with the Norwegian Paper and Fibre Research Institute, PFI.

The overall aim of the project was to enhance quality of paper produced from peroxide bleached thermomechanical pulp (TMP) as well as to improve the runnability of a paper machine using TMP. The main focus was decided to put on dissolved and colloidal substances present in white water which are known to have a major role when dealing with e.g. paper machine runnability problems and paper quality questions.

The project was divided into two parts which were carried out at the Laboratory of Forest Products Chemistry and Laboratory of Paper and Printing Technology. The former laboratory performed the fundamental surface chemistry studies and the latter the studies of sheet formation, water retention and paper properties. The latter information is not included in this thesis.

The basis of the more complex studies of TMP white water interactions using a relatively new surface sensitive technique (quartz crystal microbalance with dissipation, QCM-D) was created in **Paper I.** This was done by choosing a fairly more simple system to examine the usability of this sophisticated method in the application where papermaking components and additives are used. Paper I presents results of the system where cationic polyelectrolyte (cationic starch) was adsorbed on the oppositely charged silica surface. Three different cationic starches with varying charge densities and molecular weights were investigated. Hence, the goal was to understand the structure of the adsorbed layers, its dependence on the electrolyte concentration, polymer charge density and molecular weight distribution. The aim of Paper I was to ensure that adsorption results adhere to the well-known theories of polyelectrolyte adsorption.

Cationic starch layers were also modeled with theoretical simulations using a Voigt-based viscoelastic model in order to achieve further information about the thickness, shear elastic modulus and shear viscosity of the adsorbed film. X-ray photoelectron spectroscopy (XPS) was used as a quantitative verification method for adsorbed amounts detected with QCM-D. The XPS verifications indicate that QCM-D is an excellent and reliable method to be used in the polyelectrolyte adsorption studies. The adsorption behavior of this cationic starch on the oppositely charged silica surface was very well in accordance with the polyelectrolyte adsorption theories. Adsorption of cationic starch depended on the charge density, electrolyte concentration and molecular weight as expected.

Pulp fibers cannot be used for direct surface interaction studies on a molecular level. Therefore, substrate surfaces were to be used in the QCM-D instrument, which would model the real main fiber components. Materials for the model surface preparation were chosen so that they represent the main components present in thermomechanical pulps (cellulose, lignin and extractives. **Paper II** and **Paper III** present the preparation and characterization of these model surfaces. In Paper II the model cellulose surfaces were prepared by employing the application of Langmuir-Blodgett (LB) deposition technique from trimethylsilyl cellulose (TMSC). This rather complicated technique was chosen since similar cellulose surfaces were used earlier at our laboratory in different surface chemistry studies (Holmberg et al. 1997). The previous procedure only needed some modifications in order to apply the deposition technique on the QCM-D crystal surfaces.

In Paper III the preparation and characterization of lignin and wood extractive surfaces using spincoating technique is described. It was found that also these surfaces give highly repeatable adsorption results. Based on the atomic force microscopy

(AFM) and XPS analyses all the three model surfaces were morphologically and chemically suitable for this kind of adsorption studies conducted with QCM-D.

All the surfaces were prepared to study the affinity of dissolved hemicelluloses and colloidal extractives towards the main fibre components. In **Paper IV** dissolved hemicelluloses isolated from both unbleached and bleached TMP as well as colloidal extractives were adsorbed at different ionic strength on cellulose, lignin and wood extractives. The results achieved from Paper IV were applied to explain some observations investigated in **Paper V**. It was found in Paper V that colloidal wood extractives selectively adsorb on lignin rich flake-like fines. The reason for this behavior was assumed to be due to the differences in the hemicellulose affinities towards cellulose, lignin and extractives and due to the steric hindrance created by loosely bound hemicellulose molecules' loops and tails.

3 BACKGROUND

3.1 Some features of thermomechanical pulp

During thermomechanical pulping (TMP) process the fibers are separated from the wood by refining the chips at elevated temperature and under pressure. The middle lamella and primary wall of the cell wall are softened (mainly hemicelluloses and lignin) during the pulping process, and the fibers are separated without being damaged too much. At the same time a relatively high amount of fines material is produced (10-40% of the total pulp). Contrary to chemical pulping, mechanical pulping does not remove lignin and hemicelluloses, and all the components, cellulose, hemicelluloses, lignin and wood extractives are present in the fibers and fines (Sundholm 1999).

Norway spruce (*Picea abies*) is the most suitable soft wood species for thermomechanical pulping due to its favorable fiber properties such as fiber cell wall thickness and fibril structure. The bulk chemical composition of spruce fiber is the following: cellulose content is 40-45% of the wood dry solids, hemicellulose content is 25-30%, common lignin content is in the range of 25-30% and extractive content varies between 0.5-2% (Alen, 2000). Together with the good fiber properties, the low extractive content (0.5-2%) and high initial brightness of the wood give good strength, optical and smoothness properties to the final paper product. In addition, the cellulose rich fibrillar fines have been reported to increase the bonding properties of the paper sheet (Luukko and Paulapuro 1999). Flake-like fines have poor bonding ability, but they are shown to improve light-scattering and thereby opacity (Luukko and Paulapuro, 1999).

Lignin, which content is relatively high (30%), is the main source of colored material in thermomechanical pulp fibers (Lindholm 1999). Removal of lignin would need harsh chemical treatments and, as a consequence, the benefits of mechanical pulping would be lost. Thus, the desired pulp brightness increase is achieved by elimination of colored groups of lignin instead of lignin removal. Elimination of chromophoric structures of lignin is achieved by hydrogen peroxide or sodium dithionite bleaching.

Printing paper grades such as newsprint, uncoated SC paper and LWC magazine paper, with good opacity and printability at low basis weight, are produced using TMP. Use of low basis weights brings economical advantages especially in large volume products. On the other hand, the strength and durability of these papers are relatively limited. Mechanical pulping does not remove lignin, so over the time UV-radiation reacts with lignin making the paper yellow. Thus, the archiving properties are poor and especially uncoated grades have end uses with short life cycle.

3.1.1 TMP surface properties

The chemical surface composition of TMP fibers can differ much from the bulk composition (Wågberg and Annergren 1997). Suitable surface sensitive techniques such as XPS, AFM and ToF-SIMS (Time-of-Flight Secondary Ion Mass Spectroscopy) have been developed and applied to analyze the surfaces of TMP fibers and fines.

The surface chemical properties of TMP have been widely studied by XPS. Dorris and Grey (1978a 1978b) and Grey (1978) were the first to apply the technique to analyze the surface properties of mechanical pulps. They interpreted the C(1s) and the O(1s) peaks by the deconvolution method which determines the chemical shifts of the peak. They presented a way to estimate the weight fraction of cellulose and lignin on the fiber surface and also the influence of the extractives on the oxygen/carbon (O/C) ratio. Many different mechanical pulps were characterized with these definitions and they were able to show that lignin content of TMP fibers was higher when compared to bulk content.

The XPS evaluation of the compound depth distribution of surface lignin and extractives on TMP by Tougaard background analysis was presented by Johansson (2002). This work showed that peroxide bleached and unbleached TMP samples have similar surface lignin content. Thus, peroxide bleaching does not attack the surface lignin. The work also suggested that TMP surface is at least partially covered by a thin film of extractives.

The surface properties of TMP fine material have also been studied using XPS. According to Luukko et al. (1999) and Mosbye et al. (2003) the extractives are enriched on the surface of fines. Mosbye et al (2003) also showed that the bulk composition of the fines varied in the following way: carbohydrate content increased and the amount of klason lignin decreased as the refining proceeds. The surface of the flake-like fines (fines produced during the first refining state) is lignin and extractive rich while the fibrillar fines produced during later refining stages have less lignin and extractives on the surface (and consequently a higher carbohydrate coverage).

Since the ToF-SIMS technique provides information on the chemical structure of lignin and extractives, it completes the information achieved from XPS. The chemistry of paper surfaces studied using SIMS was demonstrated for the first time by Brinen et al (1991). ToF-SIMS together with XPS has recently been used to analyse the surface distribution of extractives on TMP sheets (Kokkonen et al. 2004). Extractive model compounds were added to an acetone extracted TMP and ToF-SIMS studies showed that the extractives were evenly distributed on the sheet surfaces. Kleen et al (2003) showed that both, fibers and fines fraction of TMP, contains more extractives, lignin and pectin than bulk fibers.

Morphological properties of the fiber surface e.g different fibre wall structures and different surface components of mechanical pulp fibres (Hanley et al. 1991, Hanley and Grey 1994, Börås and Gatenholm 1999, Niemi et al. 2002, Gustafsson et al. 2003, Koljonen et al 2003,) and fines (Kangas and Kleen 2004) can be identified using AFM imaging technique. Gustafsson et al. (2003) studied the effect of refining on TMP surface properties. AFM results revealed that independently of the process temperature, one stage refining produced structures which were indentified as S1-S3 cell wall surfaces and after two-stage refining indications of damaged microfibrills were found. At high temperature the refining resulted in fibrillar and granular structures which were identified to originate from the P/S1 cell wall interface.

AFM imaging gives also valuable additional knowledge to chemical analysis of mechanical pulp fiber and fine surfaces achieved by XPS and/or ToF-SIMS. Börås and Gatenholm (1999) showed, using AFM and XPS, that treatments such as washing, peroxide bleaching and extraction affect the CTMP fiber surface composition whereas the bulk composition is not affected. Koljonen et al. (2003) showed that by combining XPS and AFM important information about surface lignin and extractives was achieved. They concluded that mechanical pulps were covered by lignin and extractives from 50 up to 75% and especially extractives were enriched on the surface. Kangas and Kleen (2004) combined XPS, ToF-SIMS and AFM in order to study the surface properties of TMP fibers and fines (fibrillar and flake-like fines). They found that fines contained more extractives and lignin than fibers. Moreover, flakes had a high surface content of lignin and fibrillar surfaces were rich in extractives.

3.1.2 Dissolved wood polymers and colloids in TMP process waters

When thermomechanical pulp is produced, dissolved and colloidal substances (DCS) are released into the process water (Allen 1975, Holmbom et al. 1991, Thornton et al. 1994, Holmbom and Sundberg 2003) and they follow the pulp flow into the paper machine system. The carry over of the dissolved and colloidal substances is even more pronounced due to the closure of the paper machine white water systems.

The colloidal components are lipophilic extractives (wood resin) mainly consisting of fatty and resin acids, triglycerides and sterols. The term colloidal system defines the finely divided material (particle dimensions between ~1 nm - ~1 µm) dispersed in the surrounded medium (Stenius 2000). In this thesis, the colloidal system is the wood extractives in aqueous medium. Thus, other materials in other surrounding media are not further discussed here. The colloidal wood resin droplets with diameters in the range of 0.1-2 µm have essentially the same composition as the resin in the wood raw material.

The colloids remain stable as long as their affinity for the solvent remains stronger than their affinity for each other (Stenius 2000). Stability is due to a balance of attractive and repulsive interactions at interfaces. The colloidal system is electrostatically stable if the colloids can be made to coagulate by adding the electrolyte to the surrounding media. This kind of coagulation can be prevented by adsorbing polymers on colloidal particles. Polymers can create a steric hindrace around the colloids leading to very stable system due to high repulsion between adsorbed polymer layers. Sterically stabilized dispersions remain stable also at high electrolyte concentrations.

Dissolved substances are primarily soluble wood anionic or neutral hemicelluloses and pectins. Some lignans and lignin related substances are also present in the dissolved fraction.

The dominating dissolved hemicellulose in thermomechanical pulping of spruce is O-acetylgalactoglucomannan composed of mannose, glucose and galactose units in a ratio of 3:1:1. The acidic arabinogalactan composed of galactose, arabinose and glucuronic acid with a ratio of 4:1:1 contributes to the anionic charge in TMP waters, whereas the third main hemicellulose in spruce, arabino-4-O-methylglucuronoxylan, is released only in small amounts in mechanical pulping. A minor amount of pectins which are composed of galacturonic acid and rhamnose units is also present in unbleached TMP waters (Thornton et al. 1994).

The alkaline conditions during TMP peroxide bleaching change the amount and the chemical composition of the dissolved material. Hydrolytic splitting of acetyl groups in galactoglucomannan decreases the solubility of the polymer. This results in readsorption of deacetylated galactoglucomannans on the fiber surface and a decreased amount of glucose and mannose units in water phase. In addition, highly charged demethylated pectins are dissolved from the TMP, which results in a higher concentration of polyanions in waters (Holmbom et al. 1991, Thornton et al. 1994).

DCS in the process water often give rise to various problems such as deposits, growth of fungi and bacteria. Due to the anionic charge of these substances they tend to interact with cationic chemicals, such as retention aids, increasing the consumption of these. It has been shown that colloidal wood resin reduces the strength properties of paper (Brandal and Lindheim 1966, Sundberg et al. 2000, Kokkonen et al. 2002). It is suggested that the reason for strength reduction might be the decreased amount of hydrogen bonds between the fibers. Colloidal wood resin is adsorbing on the fiber surfaces and as a consequence the hydrogen bonding is prevented.

On the other hand, dissolved hemicelluloses have been found to be beneficial for paper quality. Dissolved hemicelluloses have been shown to reduce the negative effects of wood extractives on paper properties (Sundberg et al. 2000). Hannuksela et al. (2002, 2003a and b, 2004a and b) have studied the sorption of mannans on pulp fibers, how the strength properties of handsheets are improved by galactoglucomannans and galactomannans.

The adsorption of hemicelluloses on extractive colloids and their stabilizing effect on colloidal wood resin has been studied extensively (Johnsen et al. 2004, Sihvonen et al. 1998, Sundberg et al.1994a, Sundberg et al 1994b). Through these investigations, the effects of electrolytes (NaCl and $CaCl_2$) and the origin of DCS (unbleached and peroxide bleached TMP) on the stabilization of colloids by wood polysaccharides have been clarified. The steric stabilization of colloidal resin by dissolved hemicelluloses, especially galactoglucomannans (Hannuksela et al. 2004, Sundberg et al. 1996c), prevents the colloids from aggregating at the addition of salt. The stability of resin reduces its ability to form deposits (Otero et al. 2000).

In order to deal with problems related to DCS and to better understand the colloidal and polymeric interactions present in the wet end of the TMP process, the affinities of dissolved carbohydrates and colloidal extractives towards different fibrous components have been investigated in this thesis.

3.2 Surface forces

Intermolecular forces can have different effects at short and long range. Short range forces “work” at or very close to molecular contact (< 1nm), while long range forces operate at larger distances and become negligible at distances over 100 nm. Three of the most important forces between macroscopic particles and surfaces in liquids, which, hence, can be assumed to affect in the wet-end of the paper machine, are the van der Waals, electrostatic and steric polymer forces (Israelachvili 1992). Other forces, such as hydrophobic forces and Lewis acid-base interaction are not further discussed in this thesis.

The total interaction between any two surfaces combines the contributions of the short range van der Waals attraction and long range electro-osmotic double layer interaction. This approach is referred to as the DLVO theory, which predicts that at large separation the interaction will be dominated by the osmotic double layer repulsion, while at shorter distances the attractive van der Waals force becomes more important (Derjaguin and Landau 1941, Verwey and Overbeek 1948).

van der Waals forces. The van der Waals forces refer forces arising from the polarization of molecules into dipoles. This includes forces that arise from fixed or angle-averaged dipoles (Keesom forces) and free or rotation dipoles (Debye forces) as well as shifts in electron cloud distribution (London forces). The van der Waals forces depend on the chemical composition of the surface and ions and they are independent of the electrolyte concentration.

The van der Waals interaction between macroscopic particles depends on the geometry of the different bodies (Israelachvili 1992). The interaction between bodies on the basis of pairwise additivity is calculated using the Hamaker summation method, in which the energy of all the atoms in one body is summed with all the atoms in the other (Hamaker 1937). A simple expression of the non-retarded van der Waals force between the sphere and the surface is:

$$\frac{F_{vdW}(D)}{R} = -\frac{A}{6D} \tag{3.1}$$

where D is the distance between the sphere and the surface, R is a radius of the sphere and A is the material dependent Hamaker constant. The assumption of pairwise additivity ignores the influence of neighboring atoms on the interactions between any pair of atoms. Further, it is difficult to treat the effect of the medium on the pairwise additivity. The problem of additivity is avoided in the Lifshitz theory, where the atomic structure is ignored and the forces between large bodies are treated as continuous media (Lifshitz 1956). The forces are derived in terms of bulk properties such as dielectric constants and refractive indices. The van der Waals force takes the same functional form but the material dependent Hamaker constant function takes account of the bulk properties. An approximate expression for the non-retarded

Hamaker constant for phase 1 interaction with phase 2 across medium 3 can be calculated as:

$$A \approx \frac{3}{4}kT\left(\frac{\varepsilon_1 - \varepsilon_3}{\varepsilon_1 + \varepsilon_3}\right)\left(\frac{\varepsilon_2 - \varepsilon_3}{\varepsilon_2 + \varepsilon_3}\right) + \frac{3hv_e(n_1^2 - n_3^2)(n_2^2 - n_3^2)}{8\sqrt{2}(n_1^2 + n_3^1)^{1/2}\left[(n_1^2 + n_3^2)^{1/2} + (n_2^2 + n_3^2)^{1/2}\right]} \quad (3.2)$$

where k is the Boltzmann constant, T is the temperature, n_i is the refractive index, ε_i is the dielectric constant, v_e is the main electronic absorption frequency in the UV region and h is the Planck's constant.

Electric double layer forces. The surface charge is balanced by an equal but oppositely charged cloud of counterions (Israelachvili 1992). The part of the counterions, which are immediately outside the surface, is called the Stern layer, in which the short range interactions are of primary importance. The amount of counter ions decreases exponentially with distance from the charged surface and the counter-ions which are freely mobile but still affected electrostatically by the surface are forming a diffuse double layer. When two charged surfaces approach each other in an aqueous solution the double layers start to overlap, which results in an osmotic pressure, and, hence, give rise to the double layer force. This long range interaction is repulsive when the surfaces are of the same sign and is attractive between the surfaces of different signs.

The thickness of the double layer can be described by the Debye length κ^{-1}:

$$\kappa^{-1} = \sqrt{\frac{RT\varepsilon_r\varepsilon_0}{2F^2 I}} \quad (3.3)$$

where R is the molar gas constant, T is the temperature, ε_r is the permittivity of the solvent and ε_0 is permittivity in vacuum, F is the Faraday constant. I is the ionic strength, $I = 1/2\Sigma z_i^2 c_{0,i}$, where z is the valency of the ion and c is the concentration of the ion. Because κ increases with increasing electrolyte concentration, both the repulsive interaction between surfaces of the same sign and the attractive interaction between surfaces of different signs decrease when salt is added.

Steric forces. When two polymer covered surfaces approach each other, they experience a force when the outer polymer segments begin to overlap. On approach the chains have to adopt a more dense conformation and they loose some of their conformational freedom. Due to the unfavorable entropy associated with compressing the chains between the surfaces, the interacting forces are repulsive osmotic forces (Israelachvili 1992). The other important contribution to the steric force is the change in enthalpy associated with replacing polymer-solvent interactions with polymer-polymer and solvent-solvent interactions. This contribution can be either attractive or repulsive depending on polymer solubility.

3.3 Polyelectrolytes

Polyelectrolytes are polymers with ionizable groups that can dissociate in solution, leaving ions of one sign bound to the chain and counterions in solution. The most commonly occurring ionic groups are carboxylate ($-COO^-$), sulphate (SO_4^{2-}), sulphonate (SO_3^{2-}), phosphate (PO_4^{3-}), ammonium (NH_3^+) and protonated amines ($-NR_4^+$) (Jönsson et al. 1998). In papermaking polyelectrolytes are used as retention aids, fixing agents and wet and dry strength additives. Charged wood polymers, such as anionic hemicelluloses, are also liberated into the process waters during pulping and papermaking giving an additional source of polyelectrolytes present in the system. Figure 3.1 shows examples of polyelectrolytes which are widely used in papermaking.

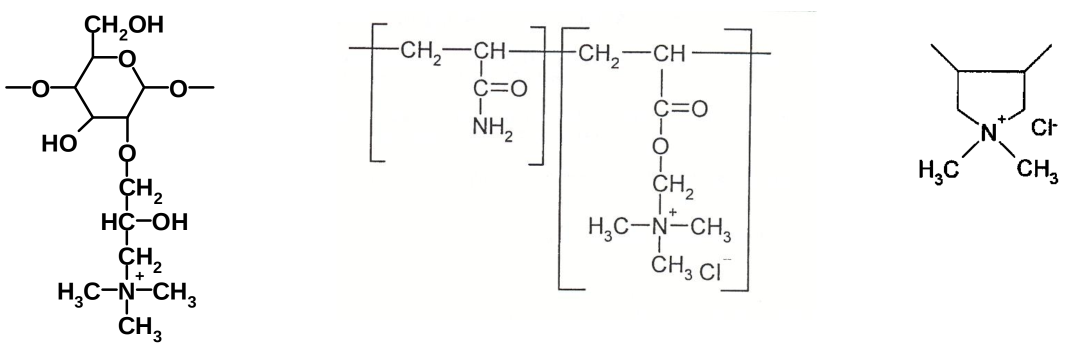

a) b) c)

Figure 3.1. Molecular formula of a) wet strength additive (cationic starch, CS), b) retention aid (cationic polyacrylamide, C-PAM) and c) fixing agent (poly-DADMAC).

Due to the dissociation in solution the polyelectrolyte system is electrically charged. Charges in the system produce a strong electrostatic repulsion, the strength and range of which depend on the linear charge density of the polymer and on the concentration of counterions in the solution.

The charge density of polymer is determined as charge per average molecular mass (meq/g), which is known as cationicity or anionicity depending upon the sign of the charge. It is a ratio of the charged groups to the total number of repeat units in the polymer (Roberts 1996). Charge of the polymer can also be described in mol-% or as a degree of substitution (DS). DS is the ratio of the number of ionisable groups in the polymer chain to the number of uncharged monomer units in the chain (Stenius 2000). DS is used only for biopolymers.

The counterions are mobile but they are influenced by the electric field created by the polyelectrolyte. Counterions form a diffuse layer, in which the ion concentration decreases from a high value close to the polyelectrolyte to bulk ion concentration at larger distances. In other words, the formed electrical field is screened by the counterions, i.e. it decays rapidly with increasing distance. The characteristic length of the decay is the so-called Debye screening length κ^{-1}, see equation 3.3.

Electrostatic repulsion between the polyelectrolyte charges has two basic effects: (i) internal repulsion which stretches the polyelectrolyte chain and (ii) intramolecular repulsion between the chains. The repulsion can be lowered by adding, for example, simple electrolyte which changes the polyelectrolyte configuration into a random coil.

The conformation of the polyelectrolyte depends mainly on the charge density and molecular weight of the polymer, the ionic strength of the solution and the surface charge density. At low ionic strength polyelectrolytes have a rod-like conformation due to intramolecular repulsion between charged segments (Liu et al. 1991). When the ionic strength is increased, the polyelectrolytes have less restricted conformations (Granfeldt et al. 1992).

The dimensions of a polymer coil are normally given by two quantities (Fleer et al. 1993, Eisenriegler 1993); the radius of gyration, R_g, and R^2, which is the mean square end-to-end distance between the ends of the chain. R_g is the root-mean-square distance of the segments from the centre of mass of the coil.

Real polymers are not able to rotate freely. C_∞ is a rigidity constant that depends on the structure of the polymer chain. It takes into account the restrictions of the rotations, e.g. valence angles between bonds and it is defined in equation 3.4.

$$C_\infty = \frac{R^2}{r l_m^2} \qquad (3.4)$$

where r is a degree of polymerization and l_m is the average length of the monomer. Expansion of the polymer chain increases with increasing R^2 and rigidity constant.

Persistence length q_t of a polyelectrolyte chain can be defined as a correlation length over which the chain loses its orientational memory. It is a distance along the chain over which the polymer maintains a stiff rodlike structure (Odijk 1978).

For a very flexible worm-like chain, the persistence length is slightly larger than the average length of the monomer. In the case of stiff rods, the persistence length convergences infinity.

For polyelectrolytes the persistence length can be divided into one non-electrostatic (q_0) and one electrostatic (q_e) part:

$$q_t = q_0 + q_e \tag{3.5}$$

Persistence length is a function of ionic strength. At high salt concentration q_t is small and the chain is flexible whereas at low salt concentration q_t is large and the chain is rigid.

3.3.1 Adsorption of the polyelectrolytes

An increase in concentration of the solute in the interfacial region is generally called adsorption. When adsorption involves the formation of a chemical bond, it is called chemisorption. The physisorption is used when only physical interactions play a role. The reduction in solute concentration near the interface is called negative adsorption or depletion in the case of polymers. Whether adsorption or depletion is found depends on the difference between the free energy of segment/surface contacts and that of solvent/surface contacts.

From a thermodynamic point of view, there are several reasons for polymers to adsorb on the surfaces:

1) Specific interaction between the polymer and the surface such as opposite charges.
2) Entropy that is gained when solvent molecules are released from the surface into solution. Entropic force favors adsorption.
3) Poor and good solvent: If polymer is only slightly soluble in the solvent, the interaction between the polymer segments and the solvent molecules is unfavorable when compared to the segment-segment and solvent-solvent interaction energy. Hence, polymer escapes contacts with the solvent and adsorbs on the surface, even on a liquid/air interface.

Theoretically, the adsorption of the polymer on the surface can be modeled on the basis of Flory-Huggins theory of phase behavior of polymer solutions (Flory 1953) and a self-consistent-field theory (Scheutjens and Fleer 1979 and 1980, Böhmer et al.

1990). There are two different types of interactions in the model: electrostatic and non-electrostatic. The non-electrostatic interaction between species in adjacent lattice sites is described by Flory-Huggins χ-parameter of polymers in solution. Parameter is the free energy change in units of kT accompanying transfer of a segment from pure polymer to pure solvents. It describes the polymer solvency into the liquid.

The adsorption mechanism of a polyelectrolyte is divided into three steps (Dijt et al. 1994): transport from the bulk to the surface, attachment to the surface and rearrangements in the adsorbed layer to minimize the surface energy.

Simply, the adsorption depends on the strength of the interaction between the polymer segment and the adsorbent surface. In polyelectrolyte adsorption the electrostatic interactions play an important role. Adsorption depends on the charge density of the polymer and the surface in the following way, see Figure 3.2:

1) Polyelectrolyte with a low charge density has a weaker repulsion between the charged segments. Conformation is more coiled and when adsorbed on the surfaces, molecules form loops and tails pointing out to the solution phase. Adsorbed amount and layer thickness are high.
2) Polyelectrolyte with a high charge density has a strong repulsion between the charged segments and the molecule adsorbs in a flat conformation. The adsorbed layer is very thin and only a small amount of the polyelectrolyte is enough to neutralize the system.

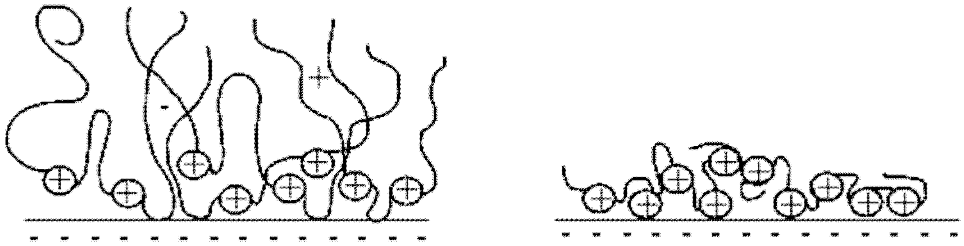

a) b)

Figure 3.2. Schematic drawing of cationic polyelectrolytes adsorbed on oppositely charged surface. a) low charge density and b) high charge density.

Increase in electrolyte concentration reduces the repulsive forces between the charged segments of the polyelectrolyte, leading to a decrease in persistence length of the polyelectrolyte. Osmotic pressure, which makes the polyelectrolyte molecule swell, decreases causing a decrease in the radius of the molecule. The surface can accommodate more molecules and, thus, the adsorbed amount increases. Increased electrolyte concentration also reduces the electrostatic attraction between polyelectrolytes and the charged surface leading to a lower adsorption at high electrolyte concentration. The driving force for adsorption at high electrolyte concentration must be non-electrostatic in nature. At very high electrolyte concentration polyelectrolyte behaves like a neutral polymer. Thus, at high electrolyte concentration polyelectrolyte can adsorb only if there is an attractive interaction between segments and a surface, which is not electrostatic.

When studying charged systems, the conformation of the polyelectrolyte affects the adsorbed amount together with molecular weight. If polymer lies flat on the surface (highly charged polyelectrolyte and/or surface at low ionic strength), there will not be any molecular weight dependence. If polyelectrolyte adsorbs in a more coiled conformation with loops and tails pointing out to the solution phase (low charged polymer and/or surface at high ionic strength) the adsorbed amount is directly proportional to the molecular weight. Increase in molecular weight increases the adsorbed amount on a smooth surface (Kolthoff and Gutmacher 1952, Chibowski 1990).

Polydispersity has also an effect on adsorption because the rate of adsorption depends on molecular weight. Adsorption of the polyelectrolytes to a solid-liquid interface can be considered as diffusion controlled transport (Brownian motion) if any liquid flow is absent (Dukhin et al. 1995, Stenius 2000). This process is determined only by molecular movements such as rotations. If the adsorption is diffusion controlled the smaller molecules diffuse faster to the surface. The surface layer may contain a larger fraction of smaller molecules even if the solution contains larger molecules as well. Small molecules reach the surface faster than bigger molecules due to the smaller friction between the polyelectrolyte molecules and solvent molecules. As time proceeds the smaller molecules can be exchanged to larger ones. Thus, in equilibrium the surface will be enriched in larger molecules.

4 EXPERIMENTAL

4.1 Materials

4.1.1 Substrate surfaces for adsorption experiments

QCM-D crystals. The sensor crystals used were AT-cut quartz crystals supplied by Q-sense AB, Gothenburg, Sweden. They are thin (0.3 mm) with $f_o \approx 5$ MHz and $C \approx 0.177$ mg m^{-2} Hz^{-1}. The crystals used in Paper I were coated with silica by means of vapor deposition. Thus, silica was always the adsorbent surface in Paper I. The sensor crystals used as a substrate for model surface preparations and in the QCM-D experiments in Papers II-V were spin-coated with polystyrene by the supplier. The polystyrene surface was hydrophobic i.e. the contact angle of pure water on the crystal surface was 95° ± 2°.

*Cellulose***.** Trimethylsilyl cellulose (TMSC) was prepared by silylation of microcrystalline cellulose powder from spruce (Fluka) with hexamethyl disilazane in the way as first suggested by Greber and Paschinger (1981) and Cooper et al. (1981). The details of the synthesis and purity check of the product conducted with FTIR are reported in Paper II. TMSC conversion to cellulose by desilylation was carried out by keeping the TMSC surface for at least 1 min in the atmosphere above a 10% aqueous HCl solution according to Schaub et al. (1993).

*Lignin***.** Lignin was isolated from Norway spruce (*Picea abies*) at KCL Science and Consulting, Espoo, Finland. The isolation of milled wood lignin (MWL) was performed using a slight modification of the Björkman method (Björkman 1956), including an ultrasonic extraction step at 15 °C.

TMP extractives. Hexane extraction of TMP extractives with a Soxhlet apparatus was performed using the procedure described by Sundberg et al. (1996b). The mixture of extractives obtained after evaporation of the hexane was dissolved in acetone and stored in a freezer. Chemical composition of the extractive mixture determined by gas chromatography (GC) (Örsa and Holmbom 1994) is shown in Table 4.1.

Table 4.1. Composition of the extractives derived from spruce TMP.

Extractives (%)	
Fatty and resin acids	26
Triglycerides	48
Steryl esters	23
Sterols	2

Flake-like and fibrillar fines. In paper V sterically stabilized wood extractive colloids were adsorbed on different types of fines and the adsorption was measured by means of the turbidity reduction of the water phase. The TMP pulp was refined and the fines were isolated using a procedure, which resulted in flake-like rich and fibrillar rich fractions of fines (Mosbye et al. 2002). The preparation and characterization of fines material is described in detail in paper V.

4.1.2 Adsorbed materials

Cationic starch. Cationic starch (CS) was synthesized from potato starch at the laboratories of Raisio Chemicals Oy, Raisio Finland. The details are given in Paper I. Three starch samples were used: one with low degree of substitution (DS), charge density of 0.5 meq/g and high molecular weight (M_w), one with high DS, charge density of 1.5 meq/g and high M_w and one with high DS, charge density of 1.5 meq/g and low M_w. Some properties of the CS samples are given in Table 4.2.

Table 4.2. Properties of cationic starch samples.

	CS_{HL} [a]	CS_{HH} [b]	CS_{LH} [c]
Weight average molecular weight[d] (Da)	8.8×10^5	8.7×10^5	4.5×10^5
Number average molecular weight[d] (Da)	4.3×10^5	3.5×10^5	2.0×10^5
Degree of substitution (DS)[e]	0.20	0.75	0.75
Charge density (meq/g)[f]	0.5	1.5	1.5

[a]High molecular weight, low DS

[b]High molecular weight, high DS

[c]Low molecular weight, high DS

[d]by SEC (Size Exclusion Chromatography)

[e]as reported by the manufacturer

[f]determined by polyelectrolyte titration (Mütek)

Dissolved hemicelluloses. Hemicelluloses were isolated from the hexane extracted TMP by using the procedure of Thornton et al. (1994a). Dissolved hemicellulose fractions were isolated from unbleached and peroxide bleached TMP and the monosaccharide content of both water solutions, analysed with GC (Sundberg et al. 1996a), is listed in Table 4.3. The fractions from unbleached and bleached TMP are anionic with a charge density of 0.51 meq/g and 1.38 meq/g, respectively, determined by cationic polyelectrolyte titration method (Mütek, 1.0 meq/l pDADMAC, $Mw < 3\times10^5$ Da).

Table 4.3. Composition of the dissolved hemicellulose fraction's monosaccharides derived from spruce TMP.

	Monosaccharides (%)	
	Unbleached	Bleached
Arabinose	2.7	3.7
Xylose	3.0	8.9
Rhamnose	3.2	9.0
Mannose	47.1	14.0
Galactose	14.3	10.6
Glucose	14.6	5.7
Galacturonic acid	14.2	46.7
Glucuronic acid	0.9	0.7
4-O-Me-glucuronic acid	0	0.6

Model hemicelluloses. Galactoglucomannan (charge density of 0.09 meq/g and weight average *Mw* of approximately 50 kDa with unimodal *Mw* distribution analysed by SEC) was isolated from the mixture of dissolved hemicelluloses by using an ultrafiltration technique according to Willför et al. (2003).

Pectin samples with a desired *Mw* compared to pectin found in spruce were prepared from commercial citrus fruit pectin (Sigma-Aldrich Chemie BmbH, Germany) by alkaline hydrolysis. The reaction mixtures were cooled down to room temperature, acidified, concentrated by vacuum rotor-evaporator and concentrates were freeze-dried. The final product has the following properties: charge density of 2.1 meq/g and weight average *Mw* of approximately 12 kDa with unimodal *Mw* distribution analysed with SEC.

Colloidal wood extractives. In order to prepare the aqueous dispersion of colloidal wood extractives, the acetone dissolved extractive mixture was further treated as described in Sundberg et al. (1996b). As a result, a stable colloidal dispersion with an average particle size of 200-300 nm measured with N5 Submicron Particle Size Analyzer, Miami, USA, is achieved. Note that the chemical composition of the extractive model film used as a substrate surface in the QCM-D experiments is the same, see Table 4.1.

All other chemicals were of p.a. grade if not otherwise specified.

4.2 Methods

4.2.1 Adsorption experiments

Quartz Crystal Microbalance with Dissipation (QCM-D). The QCM-D technique, Q-Sense, Gothenburg, Sweden, which was the main method of investigation, is a relatively recently developed method for in-situ adsorption studies at the solid/liquid interface (Rodahl et al. 1995). The instrument consists of a thin quartz disc sandwiched between a pair of electrodes. Due to the piezoelectric properties of quartz, it is possible to excite the crystal to oscillation by applying an AC voltage across its electrodes. The principle of the measurement is the following: Without adsorbate the crystal oscillates at a resonant frequency f_o, which is lowered to f when material adsorbs on the surface of the crystal. The instrument measures the shift in the frequency of the fundamental resonance and several overtones. If the material adsorbed is evenly distributed, rigidly attached and small compared to the mass of the crystal, the shift in the resonant frequency is related to the adsorbed mass by the Sauerbrey equation (Höök et al 1998):

$$\Delta m = -\frac{C\Delta f}{n} \tag{4.1}$$

where Δm is the adsorbed mass per unit surface, $\Delta f = f - f_o$ is the frequency shift, n is the overtone number (in the present case n = 1, 3 or 5 (D300 system) and n = 1, 3, 5, 7, 9, 11 or 13 (E4 system)) and C is a constant that describes the sensitivity of the device to changes in mass.

The resonant frequency of the crystal depends on the total oscillating mass, including water coupled to the oscillation. By measuring several frequencies and the dissipation it becomes possible to determine whether the adsorbed film is rigid or water-rich (soft) which is not possible by looking only at the frequency response. If the adsorbed material is not fully elastic, frictional losses occur that lead to a damping of the oscillation with a decay rate of amplitude that depends on the viscoelastic properties of the material. With the QCM-D instrument the change in the dissipation factor, $\Delta D = D - D_o$, when material is adsorbed can be measured. D_o is the dissipation factor of the pure quartz crystal immersed in the solvent and D is the dissipation factor when material has been adsorbed. D is defined by

$$D = \frac{E_{diss}}{2\pi E_{stor}} \tag{4.2}$$

where E_{diss} is the total dissipated energy during one oscillation cycle and E_{stor} is the total energy stored in the oscillation.

QCM-D experiments. Two different set ups of the QCM-D instruments were used in the experiments, Qsense D300 system and Qsense E4 system. In the D300 system the definite volume of sample (0.5 ml) is introduced onto the crystal via temperature control loop and the changes in frequency and dissipation at 5 MHz and its overtones (15, 25 and 35 MHz) are followed as a function of time. The measurement chamber of the E4 system is specifically designed for controlled flow measurements. Samples are pumped through the measurement cells (4 parallel cells performing concomitantly) with the peristatic pump with a flow rate of 0.1ml/min. The changes in frequency and dissipation are followed as a function of time at 5 MHz similarly as with the D300 system but also at higher overtones (15, 25, 35, 45, 55 and 65 MHz). It was noticed that the adsorption experiments of the colloidal wood extractives needed to be conducted in continuous flow due the depletion of the colloids in the solution near the substrate/liquid interface when the flow was absent.

Figure 4.1 shows an example of the data achieved from the QCM-D instrument. The negative frequency change i.e. positive mass change on the crystal surface and the change in dissipation are followed as a function of time. The sample is introduced onto the crystal surface after the zero baselines for both, frequency and dissipation changes, are attained. In Figure 4.1, the sample is introduced onto the crystal at the time of 30 min.

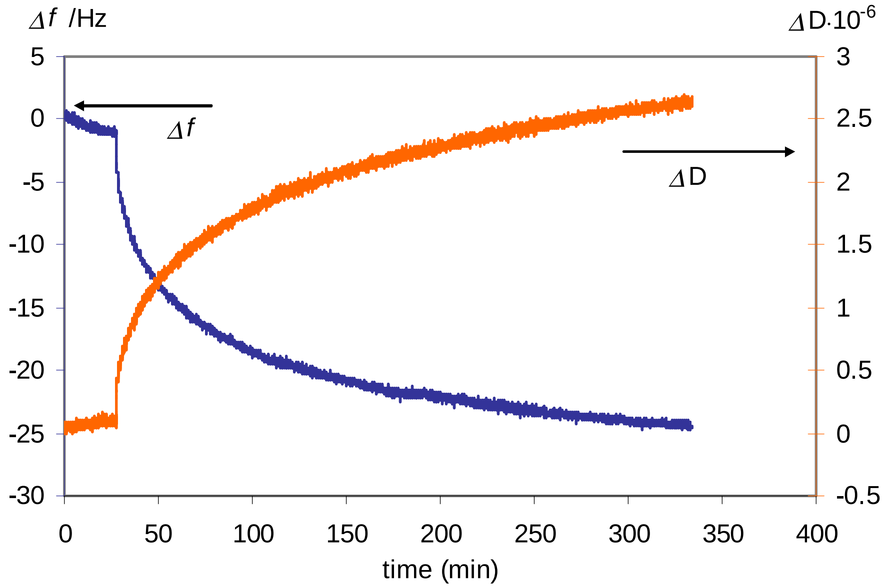

Figure 4.1. Change in frequency and dissipation as a function of time for adsorption of 100 ppm dissolved hemicellulose solution isolated from unbleached TMP in 10 mM NaAc/HAc buffer at pH 5.6 on lignin.

The frequency and dissipation responses also depend on the density and viscosity of the bulk liquid. Very sharp changes in frequency and dissipation are observed when the electrolyte concentration is changed during the measurement, see for example Figure 9 in Paper II. This so called bulk effect is a commonly known effect when using QCM-D. In this work the baseline stabilization prior to sample addition onto the crystal is conducted at the same ionic strength in order to avoid liquid peaks. The following values for the frequency and dissipation changes are measured for the quartz crystal when pure water is replaced by 100 mM NaCl: $\Delta f_{15\ \mathrm{MHz}}$ = ~-8 Hz and $\Delta D_{15\ \mathrm{MHz}} = 1.2 \times 10^{-6}$. The instrument and the crystals are regarded as fully stabilized when the detected changes in frequency and dissipation are smaller than the maximum drift of the instrument which is 2 Hz/h and 0.2×10^{-6}/h at 15MHz (Q-Sense 2000).

Details of the QCM-D experiments of each case are described in Papers I-V.

Interpretation of viscoelastic properties. Materials, which can display either viscous or elastic properties at the same time, are called viscoelastic. Polymers are a typical example of viscoelastic material. The rheological properties of polymeric material depend on the shear rate, molecular weight, the structure of polymer molecule and temperature (Barnes et al. 1989, Ferry 1980).

Using appropriate models, the QCM-D data, Δf and ΔD, can be interpreted in terms of adsorbed mass and structural changes in the adsorbed layer. In this work, the so-called Voigt based representation of a viscoelastic solid is used (Voinova et al. 1999). The Voigt model (Figure 4.2) consists of a spring and a dashpot filled with viscous fluid connected in parallel. The extension or strain in the spring is at all times equal to the extension or strain in the dashpot. The total stress in the Voigt element is equal to the sum of the stresses in the spring and dashpot (Barnes et al. 1989).

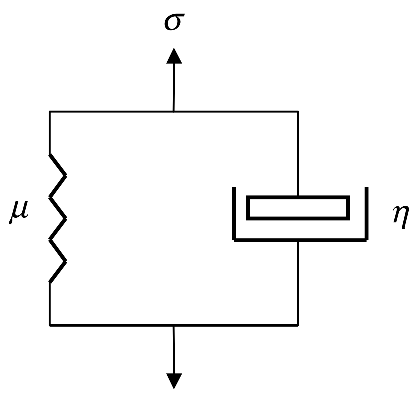

Figure 4.2. Voigt element. μ is shear modulus, η is shear viscosity and σ is shear stress (Voinova et al. 1999, Barnes et al. 1989).

Adsorbed layer, which is modeled with Voigt element, is described using a frequency dependent complex equation when the layer is subjected to oscillating stress:

$$G^* = \text{complex rigidity modulus} = G' + iG'' = \mu_f + i2\pi f\eta_f \qquad (4.3)$$

where μ_f is the elastic shear (storage) modulus, η_f is the shear viscosity (loss modulus) and f is the oscillation frequency.

The real part of the complex modulus (storage modulus) characterizes the stored elastic energy. It expresses the elastic behavior of the material and its ability to store energy. Storage modulus correlates to the stiffness or flexural modulus of the material. At constant stress higher strain yields lower storage modulus and lower strain yields higher storage modulus. The imaginary part of the complex modulus (loss modulus) characterizes the energy which changes in to heat through relaxation. It expresses the viscous behavior of the material and it is a measure of the material's ability to dissipate energy. The larger the value of the complex shear modulus, the stronger the structure of the polyelectrolyte film is.

In this study the modeling of the viscoelastic properties of the formed polyelectrolyte films was performed using the program QTools from Q-Sense (Paper I and Tammelin et al. 2006). The adsorbed film is assumed to have a uniform thickness (d_f) and a uniform density (ρ_f). The adsorbed film is situated between the QCM-D electrode and a semi-infinite Newtonian liquid under no-slip conditions; see a schematic illustration in Figure 4.3.

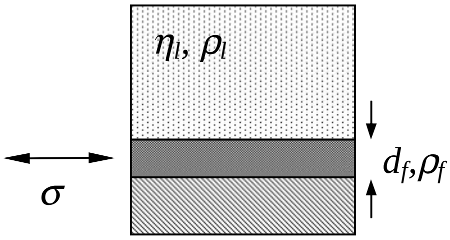

Figure 4.3. Schematic drawing of the quartz crystal covered with a viscoelastic thin film (density ρ_f and thickness d_f) in contact between the sensor surface and bulk solution. The film is represented by elastic modulus, viscosity and density. The bulk liquid is represented by density and viscosity (Voinova et al. 1999).

In practice, when conducting the QTools modelings the following parameters are used and modeled:

- Known parameters: fluid viscosity and density (η_l and ρ_l), Δf and ΔD
- Estimated parameter: Density of the adsorbed layer (ρ_f)
- Modelled parameters: Elastic modulus (μ_f), viscosity (η_f) and thickness (d_f) of the adsorbed layer

The other simple linear viscoelastic model is the Maxwell (Barnes et al. 1989) model which is not used in this study and, therefore, is not further discussed. The mechanical models always represent linear deformations in which the stress and deformation are proportional to their time derivatives. The idea of the mechanical models is not to describe polymer morphology in detail, but model the interphacial behavior in a phenomenological manner.

4.2.2 Model film preparation

Langmuir-Blodgett (LB) technique. In Langmuir-Blodgett technique relatively water insoluble compounds can be made to form a monolayer at a water/air interface. This monolayer can then be transferred onto a subsequent solid substrate. This old technique, first introduced by Irving Langmuir (Langmuir 1917) and extensively used and developed by Katharine Blodgett (Blodgett 1935), is mainly applied for preparing monolayers of the amphiphilic compounds. Good textbooks, e.g. Roberts (1990) and Petty (1996), are available related to the technique.

In this work model films of cellulose were produced using LB-equipment consisting of a computerized minitrough with two movable barriers and a device for measuring the surface pressure π (Paper II). Surface pressure is the difference in the surface tension of the pure subphase (water) and the subphase in the presence of a monolayer.

The insoluble component (trimethylsilyl cellulose, TMSC) is dissolved in a volatile solvent (chloroform), which has to have a positive spreading coefficient when spread on the water surface in order to achieve a full coverage to all available water surface. After evaporating the solvent, only the known amount of insoluble component remains at the water surface. The barriers, which are at first far apart, will then be moved towards each other in order to reduce the surface area and to compress the insoluble molecules to form a continuous film. During the film compression the surface pressure is continuously recorded by means of the Wilhelmy method (Roberts 1990), and as a result a surface pressure versus molecular area (π-A isotherm) can be determined. An example of the cellulose film π-A isotherm is shown in Figure 4.4.

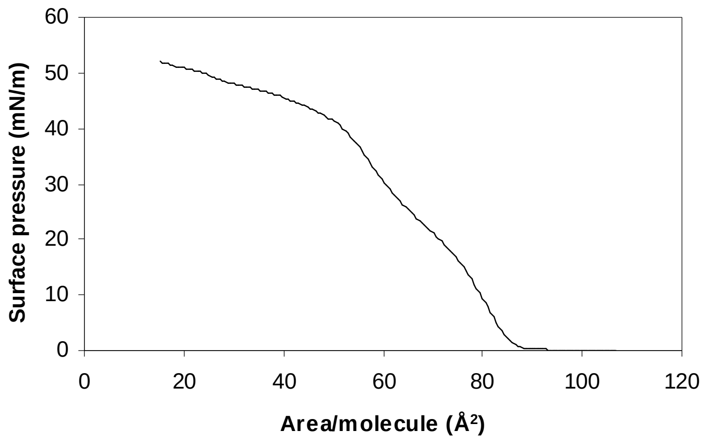

Figure 4.4. Langmuir isotherm of TMSC on water.

From the isotherm curve the molecule arrangements at the water surface can be estimated. Molecules start to organize a film when the surface area is decreased by the moving barriers. The film is at its strongest and best oriented when the curve slope has its steepest region. At higher surface pressures the slope becomes more gentle, indicating a collapse or disruption of the film. It is more straightforward to identify different molecular arrangement from the isotherm of the small surface active compounds due to their more flexible structure. The stiff and large cellulose polymer can not form as dense film on the water surface as small surfactants (a very steep rise in the curve is not detected). From the π-A isotherm the desired surface pressure is chosen to carry out the depositions to a solid substrate (in this case 15 mN/m). Surface pressure is then kept constant through the entire deposition process.

Traditionally, the substrate is dipped vertically through the floating monolayer and every time the substrate passes through the air/water interface, a monolayer is transferred on to a solid substrate. In this work the horizontal dipping procedure, was used due to the limitations originating from the structure of the QCM-D crystals. In order to obtain a monolayer, the horizontal dipping technique has been used to deposit e.g. urease (Langmuir and Schaefer 1938) and polymerized diacetylene (Day and Lando 1980). In contrast to monolayer deposition, Lee et al. (1992) first reported the bilayer deposition. In this horizontal dipping procedure, the substrate is pressed into contact with the liquid interface and it never traverses the floating monolayer. Theoretically, a bilayer of the film is formed when the substrate is withdrawn and the liquid and substrate are separated. Figure 4.5 schematically describes the horizontal dipping procedure of the TMSC on the polystyrene coated QCM-D crystal.

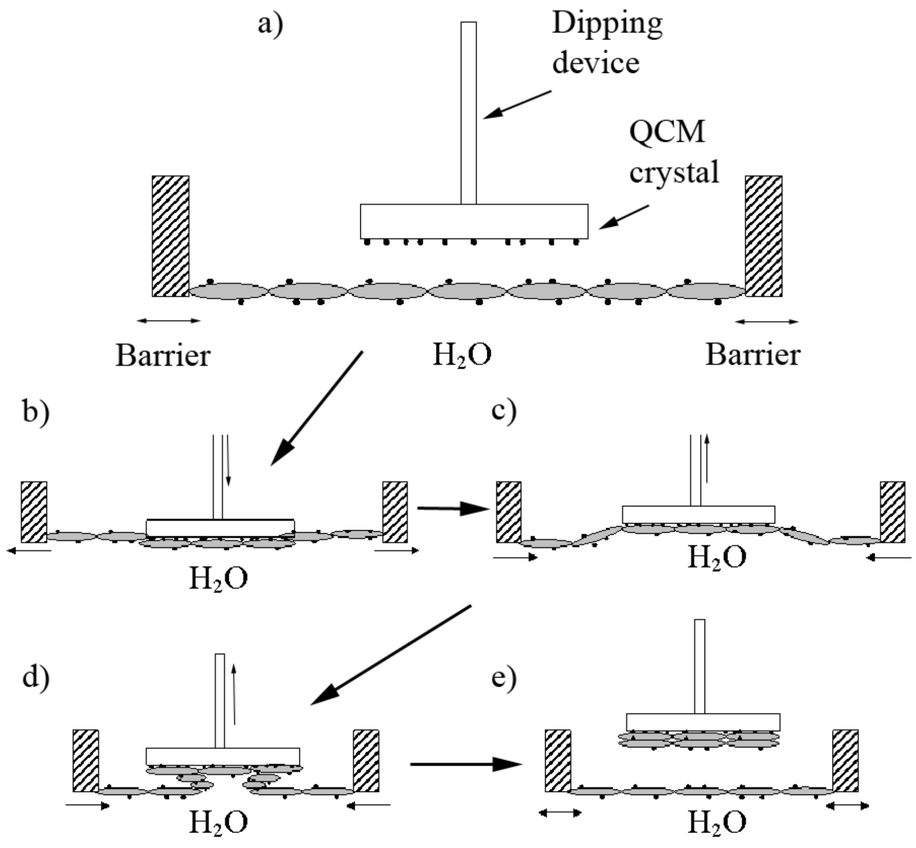

Figure 4.5. A schematic drawing of the horizontal dipping procedure. The horizontal arrows represent the barrier movements and the vertical arrows represent the movements of the dipping device during one dipping cycle. The ovals illustrate the TMSC molecules and black spots illustrate the hydrophobic parts of TMSC and polystyrene.

During the deposition process the transfer ratio is also monitored in order to verify the successful deposition. The ratio is defined as the ratio between the decrease in the floating monolayer area during the deposition and the transferred monolayer area on the solid substrate. In vertical dipping the optimal transfer ratio value is 1 (fully covering monolayer is transferred onto solid substrate surface), while the value is 2 with horizontal orientation (bilayer formed during pressing and withdrawing).

Spincoating. In spincoating technique the film is deposited on the solid surface from volatile solvent by spinning the surface with high speed. Spincoating is a simple and fast technique to prepare thin films in a repeatable manner. The equipment needed include a chuck which spins at a desired rate (500-6000 rpm) and a pump to create vacuum in order to adhere the substrate surface on the chuck. The film formation, its thickness and roughness can be controlled by varying parameters such as solution concentration, solvent properties, spinning speed, acceleration and spinning time (Meyerhofer 1978; Sukanek 1991; Bornside et al. 1993). In this work MWL lignin and TMP extractive films were prepared using spincoating technique (Paper III). The primary aim was to obtain sufficiently smooth and fully covering films of lignin and extractives, which would work well in the QCM-D instrument. Therefore, too much attention was not paid in this work to elucidate how film properties change by varying the parameters mentioned above.

4.2.3 Surface characterization

Atomic Force Microscopy (AFM). In this work the atomic force microscopy (Binnig et al. 1986) was used for imaging purposes in order to achieve information about the surface morphology of the model adsorbent surfaces (Papers II and III) and to obtain additional information of the surface properties after adsorption experiments. In a simplified manner, the height profile of the sample surface is measured by scanning the surface with a sharp tip which is attached to a cantilever. The forces between the surface and the tip affect the cantilever which acts as a spring. When a laser beam is directed onto the cantilever, the deflection of the cantilever can be detected from the laser beam with a photo detector. The sample itself is placed on a piezoelectric scanner, which is used to move the sample in x-, y-, and z-direction.

The AFM measurements were performed with a Nanoscope IIIa Multimode scanning probe microscope (Digital Instruments Inc., Santa Barbara, CA, USA). The images were scanned in tapping mode (Martin et al. 1987, Zhong et al. 1993) in air in order to avoid the sample deformation when imaging polymeric materials such as cellulose and lignin. The other AFM modes (e.g. non-contact and contact modes) are not handled in this thesis since only the tapping mode was used, and the reader is referred to e.g. Albrecht et al. (1991) and García and Pérez (2002) for further details.

The silicon cantilever (Pointprobes, type=NCH, delivered by Nanosensors) was oscillated near its resonance frequency (≈ 270-315 kHz) with the free amplitude (A_0) of about 20 nm and a set-point ratio (r_{sp}) between 0.4-0.6. The set-point ratio is the ratio between the set-point amplitude (A_{sp}) and free amplitude. In tapping mode the frequency of the oscillation is kept constant and the changes in amplitude are monitored. During each oscillation cycle the tip is in brief contact with the sample surface and the forces between the sample and tip affect the tip and a reduction in amplitude is detected. When scanning the sample, the set-point amplitude, i.e. the amplitude of the cantilever when the tip is in contact with the sample, is kept constant by moving the sample in z-direction with the piezo. By this way it is ensured that the tip to sample distance remains constant and that the forces exerted on the tip are also similar all the time. By detecting the adjusted piezo movement, a high resolution height image is recorded.

The oscillation of the cantilever is assumed to be harmonic as well as the oscillation of the piezo, which is used to vibrate the cantilever when the tip is not in contact with the sample. Harmonic motion is described by the following equation:

$$A(t) = A_0\cos(\omega t+\delta) \qquad (4.4)$$

where A_0 is the maximum amplitude during the cycle of oscillation, $\omega=2\pi f$, f is the frequency, t is time and δ is phase shift angle of the freely oscillating cantilever and piezo. The phase angle between the two oscillating motions, tip and driving force (piezo), is initially set to 90°. When the tip approaches the sample, the amplitude reduces due to the tip-sample interactions and the whole standing wave of the harmonic motion is affected. The phase angle of the harmonic waves change and this shift is recorded when the sample is scanned with the tip. Thus, the phase shift image is achieved and the additional information of sample properties, such as different elasticities or e.g. adhesive properties is recorded at the same time as the height image. In this work the energy applied to the sample is low (A_0 is small and r_{sp} is large) indicating that the phase shift is due to the chemically different regions in the sample surfaces. The differences in sample stiffness in phase image are achieved by using high A_0 and small r_{sp} (Spatz et al. 1997, Bar et al.1997)

X-Ray Photoelectron Spectroscopy (XPS). Coverage and chemical composition of the model surfaces of cellulose, lignin and wood extractives (Papers II and III) as well as the nitrogen content of the adsorbed cationic starch films (Paper I) were determined using XPS, also known as Electron Spectroscopy for Chemical Analysis (ESCA). The sample in a high vacuum is irradiated with X-rays and the kinetic energies of the emitted photoelectrons are measured (Briggs and Seah 1990). The kinetic energy of the photoelectrons depends on the binding energy to the relevant atom where the photoelectron originates from:

$$E_k = h\upsilon - E_b - \Phi \qquad (4.5)$$

where $h\upsilon$ is the energy of the X-ray, E_b is the binding energy of the photoelectron and Φ is the spectrometer dependent work function. Any element except hydrogen can be detected and the elemental analysis is highly sensitive. The ratio of elements on the sample surface is detected and the detection limit is approximately 1 atomic %. Atoms of the same element emit photoelectrons with different bonding energies depending on the local environments of the atom. Thus, the different chemical states of the element, e.g. oxidation states of metals or different bonding of the organic carbon, can be determined from the XPS spectrum.

When photoelectrons pass through a solid material, they interact with the material and can travel only a very limited distance. Thus, the intensity of escaping electrons decreases with increasing analyzing depth. As a consequence, the XPS is a very surface sensitive technique. The major part of the information in the spectrum is gained from the depth of 3 nm from the surface although the maximum analysis depth for polymeric material is reported to be 6-12 nm (Ashley and Williams 1980).

The XPS measurements were performed with a Kratos Analytical AXIS 165 electron spectrometer using a monochromated A1 Kα X-ray source. The experiments were carried out on dried QCM-D crystal samples, according to the standardized procedure developed for cellulosic materials (Johansson et al. 1999; Johansson 2002; Koljonen et al. 2003).

Figure 4.6 presents the XPS survey spectrum recorded from a layer of cationic starch adsorbed on silica surface, showing peaks due to emission of C1s, O1s, N1s, Si2s and Si2p electrons. The Auger electrons are electrons originated from higher energy levels in the atoms. C1s (carbon), O1s (oxygen) and N1s (nitrogen) originate from cationic starch film and the Si2s and Si2p (silica) originate from underlying SiO_2 surface. In this work the N1s trace analysis was used to analyse the surface content of the nitrogen in order to verify the starch adsorptions. The XPS starch investigations are discussed in more detail in Paper I.

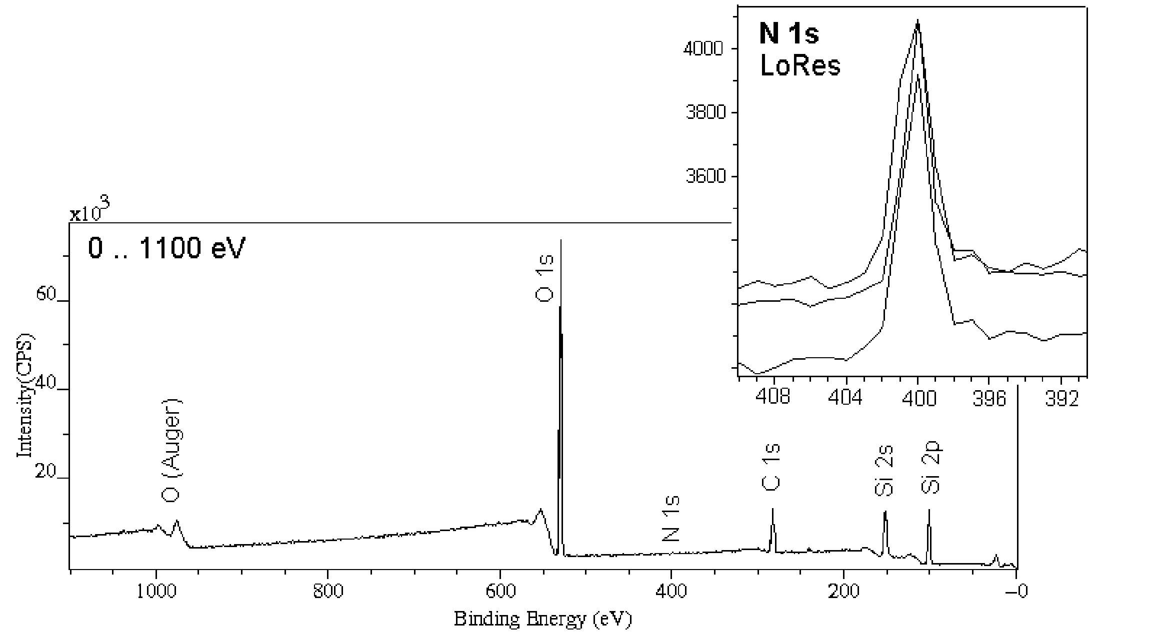

Figure 4.6. XPS survey spectrum recorded on the sample of cationic starch adsorbed on SiO_2. The excerpt shows the enlargement of the N1s peak of three different measurements in the same sample.

An example of the chemical shifts of organic carbon detected from starch film is shown in Figure 4.7. Three distinct peaks can be resolved from high resolution C1s XPS spectrum by curve-fitting of three symmetric Gaussian peaks. Three different chemical environments of carbon can be detected from starch layer: saturated hydrocarbons with bonds to other carbon or hydrogen only (C1), carbons with one bond to oxygen (C2) and carbons with two bonds of hydrogen (C3).

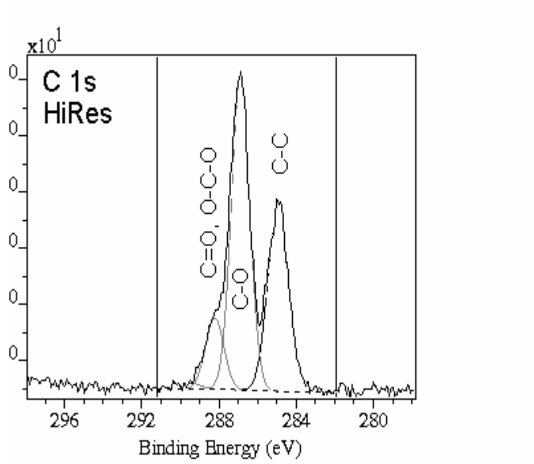

Figure 4.7. Curve resolved XPS spectrum of the C1s for the adsorbed cationic starch layer.

5 RESULTS AND DISCUSSION

5.1 Introduction of the QCM-D technique to papermaking applications (Paper I)

The groundwork to this research was done by introducing the QCM-D method to carry out the adsorption studies of the cationic starches onto the oppositely charged silica surface. The aim of Paper I was to ensure that adsorption results of cationic starch follow the well-known theories of the polyelectrolyte adsorption. In the following the adsorptions of three different cationic starches with varying degrees of substitutions and molecular weights on anionic silica surfaces were investigated. The properties of the starch samples are shown in Table 4.2. Moreover, the viscoelastic properties of the formed starch layers were analyzed using the Voigt-based viscoelastic model for solid material, see Figures 4.2 and 4.3.

Adsorption of polyelectrolyte on the oppositely charged surface is mainly driven by electrostatic interactions. Adsorption of polyelectrolyte is profoundly affected by the charge density of the polymer and the ionic strength. At high electrolyte concentration polyelectrolyte can adsorb only if there is an attractive interaction between segments and a surface which is not electrostatic. At low electrolyte concentration the adsorbed amount hardly depends on molecular weight. At high electrolyte concentration when the electrostatic interactions are screened, the molecular weight, polydispersity and the size of the molecule have a strong effect on the adsorption of the polymer (Eisenriegler 1993, Fleer et al. 1993, Dukhin et al. 1995, Jönsson et al. 1998). The adsorption of cationic starch on the anionic silica surface is a typical example of electrostatically driven adsorption. This has already been shown by several authors (Marton and Marton 1976, Wågberg and Ödberg 1989, van de Steeg et al. 1993). QCM-D technique is shown to be an adequate technique to examine the effect of electrostatics on polyelectrolyte adsorption. Plunkett et al. (2003) showed that adsorbed amount of polyelectrolyte increases with decreasing charge density of the polymer. At the same time the structural changes (monitored using dissipation response) of the adsorbed layer varied as expected: highly charged polyelectrolyte formed a flat layer with no water coupled in its structure and with decreasing charge density of the polymer, the more extending loops and tails were formed. These results were supported with XPS.

5.1.1 The effect of electrostatics

To study the effect of electrostatics two starch samples with different charge densities were used: 1) starch with a low degree of substitution (DS=0.2, charge density = 0.5 meq/g) and 2) starch with a high degree of substitution (DS=0.75, charge density = 1.5 meq/g). Both samples showed a narrow molecular weight distribution (Figure 1 in Paper I).

The changes in frequency and dissipation at the adsorption equilibrium for 100 ppm starch solutions with different charge densities at different electrolyte concentrations are shown in the Table 5.1.

Table 5.1. The final change in frequency and dissipation at different electrolyte concentrations for 100 ppm starch solutions. Adsorbed mass is calculated from eq. (4.1). f_0=5 MHz, n=3

NaCl mM	DS=0.2, M_w = 8.8×10^5 Da narrow Mw distribution			DS=0.75, M_w = 4.5×10^5 Da narrow Mw distribution		
	Δf Hz	$\Delta D \cdot 10^{-6}$	Δm mg m^{-2}	Δf Hz	$\Delta D \cdot 10^{-6}$	Δm mg m^{-2}
0	-10.5	0.14	0.62	-6.0	0.06	0.35
1	-24.2	0.42	1.43	-6.4	0.23	0.38
100	-100	5.94		-73.7	4.21	

The maximum adsorbed amount of a polyelectrolyte should be the lower, the higher its charge density is, because less polymer is required for charge neutralization and the adsorbed layer is flatter. This is the case with cationic starch adsorptions when starch samples with different charge densities are compared. Without any added electrolyte cationic starch adsorbs on the anionic silica in a flat conformation and the detected amount is very small. The adsorbed layers are thin, rigid and fully elastic ($\Delta D < 1\times10^{-6}$) and the adsorbed amount can be calculated using the Sauerbrey equation (eq. 4.1).

Addition of simple electrolyte reduces the persistence length so that more polymer fits on the surface and adsorption increases. Addition of simple electrolyte screens intramolecular repulsion between polymer segments (the persistence length of the polymer decreases) and polymer/surface interactions. Hence, the conformation of the adsorbed polymer becomes less extended and the polymer forms a thicker layer. Finally, polymer/surface interactions become so weak that the polymer does not adsorb at all unless there are sufficiently strong non-electrostatic interactions that promote adsorption. The cationic starch behaves exactly in this way and the results comply with the theory (Fleer et al. 1993 and Jönsson et al 1998).

As shown by Table 5.1, the adsorption of starch increases with increasing ionic strength independently of the charge density of the polymer. The frequency and dissipation changes resulting from adsorption in 100 mM NaCl are substantially higher than those at lower ionic strength. The change in dissipation is high ($4–6\times10^{-6}$) and non-linear (see Figure 5 in Paper I), which indicates that the formed starch layer is soft and less rigidly attached. Starch is adsorbed in a more coiled conformation forming loops and tails pointing out to the solution phase. The layers are viscoelastic and, hence, the Sauerbrey equation is no longer valid and properties of the formed layers can be analyzed in terms of the Voigt model.

The XPS investigations of the adsorbed amounts of cationic starch support the QCM-D results above. Two measured values of the amount of the adsorbed polymer were extracted from XPS spectra of dried adsorbed layers on the QCM-D crystals: the percentage of nitrogen atoms and the relative abundance of C-O bonds, see the examples of XPS survey scans and curve resolved fittings of C1s peak of cationic starch on silica surface in Figures 4.6 and 4.7. The relative abundance of C-O bonds (C1) is taken as a measure of the amount of carbohydrate in the layer and the amount of nitrogen is originated from the cationic trimethylammonium substituent of the starch. These measures give qualitative approximations of the adsorbed starch amount on the silica surface.

Figure 5.1 shows the amounts (at-%) of nitrogen and the relative abundance of C-O bonds in the adsorbed layers of cationic starch with different charge densities at different electrolyte concentrations.

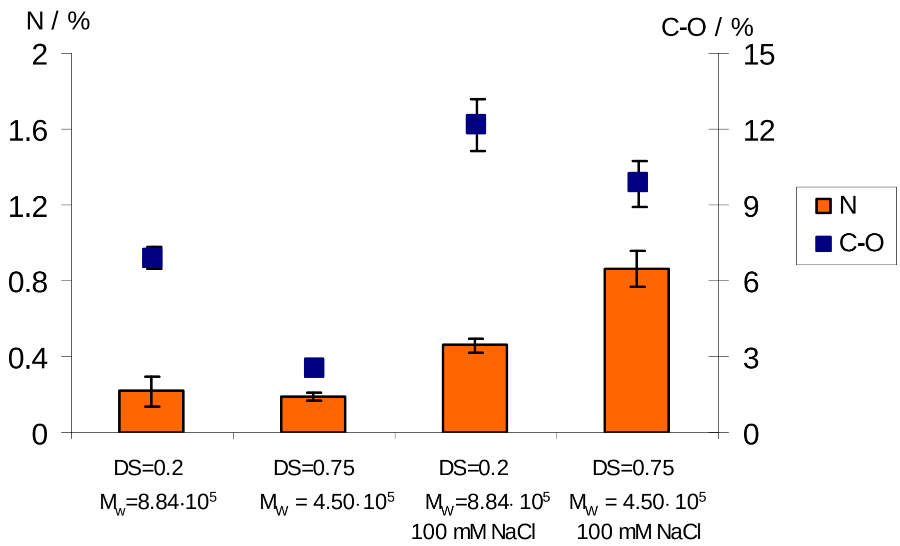

Figure 5.1. The amounts of nitrogen and relative abundance of C-O bonds (atom %) in the adsorbed layers of cationic starch analyzed by XPS. The inaccuracy of the measurements was estimated with the confidence level of 95% assuming that measurements were normally distributed.

The nitrogen content of the starch layers without any electrolyte added is 0.18 at-% for both polymers, while the amount of C-O bonds is about three times higher for starch with low charge density. The XPS results for adsorption from 100 mM NaCl solutions are also qualitatively in agreement with the QCM analysis. More starch (mg/m^2) is adsorbed on silica surface when low charge density starch is used or the electrolyte concentration is increased. Starch film also seems to be uniformly attached onto the surface; the standard deviation of the results is fairly low.

Table 5.2 summarizes the results based on the Voigt model. The deeper explanation of the modeling and the drawbacks of the model used are given in Paper I. Note that the concentrations of the starch samples are only 1/10 of those in Table 5.1. The modelings with QTools succeeded better due to slower adsorption process when more diluted samples were used since more Δf and ΔD values were recorded especially in the beginning of the adsorption process. The more data for QTools to fit, the better was the fitting result and no discontinuities were detected.

Table 5.2. Summary of the effects of cationic starch properties on adsorption and viscoelastic properties of the formed starch layer. η_f is the shear viscosity, μ_f is the shear modulus, τ_f is the relaxation time and h_f is the hydrodynamic thickness.

	DS=0.2, M_w = 8.8×10^5 Da narrow Mw distribution	DS=0.75, M_w = 4.5×10^5 Da narrow Mw distribution
$\Delta D/\Delta f$ (10 ppm)	36.4	48.0
C-O / %	12.2 ± 0.2	9.8 ± 0.9
N / %	0.46 ± 0.04	0.86 ± 0.09
η_f / Nsm^{-2}	(1.8 ± 0.3)·10^{-3}	(1.6 ± 0.1)·10^{-3}
μ_f / Nm^{-2}	(230 ± 47)·10^3	(160 ± 28)·10^3
τ_f / ns	7.8	10
h_f / nm	6.9 ± 0.2	5.1 ± 0.1

As incorrectly stated in Paper I, the starch with low charge density does not form a less weakly bound layer when compared to a starch layer of high charge density. Both values, shear viscosity (η_f) and shear elastic modulus (μ_f), are slightly higher for starch with low charge indicating a stronger layer formed on silica surface. Furthermore, the relaxation time (τ_f), which indicates how quickly the energy is dissipated under the action of forces, is lower, indicating rather a packed structure.

Two explanations can be given to clarify the observations. First, at high ionic strength the intermolecular repulsion between starch molecules is effectively screened and starch molecules can easily pack and form a dense and thick layer when using starch with low charge density. The repulsion between molecules is more pronounced with highly charged starch and in 100 mM NaCl concentration all the effects from charge density are not swamped out. As a consequence, a more mobile layer is formed. The other explanation may be due to the differences in the molecular weights. The network formed by long polymer molecules without any or fairly low repulsion between the chains is stronger when compared to a network built up by shorter chains in the presence of strong repulsion between the chains.

The explanation of the repulsion between the starch chains is supported by the findings achieved when starch adsorptions were conducted from very high electrolyte concentration (500 mM), see Table 7 in Paper I). A more mobile and weakly bound layer is formed with the starch with low charge density seen as reduced shear viscosity and shear elastic modulus values and increased relaxation times, while the estimated thickness remains the same ($h_f \approx 7$ nm). The highly charged starch behaves completely in the opposite way. Water is expelled from the film structure and a stronger and better packed layer is formed due to screened intermolecular repulsion. Because of the high charge of the starch, the electrostatic attraction towards silica is still predominant and the polymer is still strongly bound on the surface.

An observation that merits further investigation is that the adsorption of starch, even with lower charge density, is not prevented at high electrolyte concentrations. Apparently also non-electrostatic attraction is sufficiently strong to induce adsorption. Moreover, at high ionic strength the solubility of the polyelectrolytes is decreasing which promotes the adsorption and the total entropy of the system also increases when the polymer adsorbs at interfaces.

5.1.2 The effect of molecular weight

To study the effect of molecular weight on the polyelectrolyte adsorption two starches with narrow molecular weight distributions were compared: 1) the low charge density starch had a weight average molecular weight of 8.8×10^5 Da and 2) the *Mw* of the highly charged starch was 4.5×10^5 Da. Molecular weight distributions of the starch samples analyzed with SEC are shown in Figure 1 in Paper I.

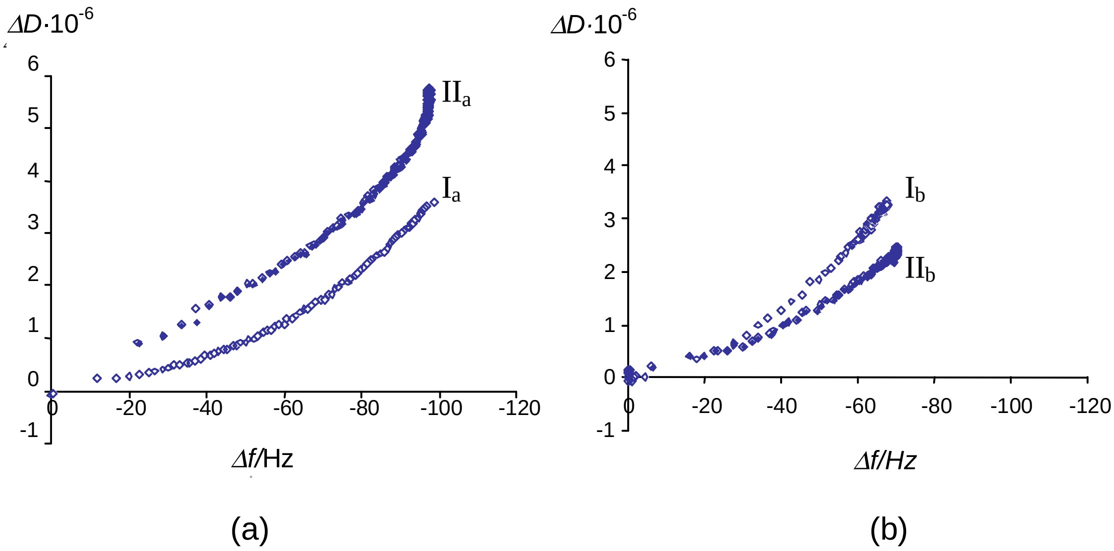

Figure 5.2. Change in dissipation factor as a function of the change in frequency for adsorption of a) 10 ppm CS (DS=0.2) solutions and b) 10 ppm CS (DS=0.75) on a silica surface. Curves I_a and I_b are starch in 100 mM NaCl and curves II_a and II_b are starch in 500 mM NaCl. f_o = 5 MHz, n=3.

When studying charged systems, the conformation of the polyelectrolyte affects the adsorbed amount together with molecular weight. If polymer lies flat on the surface there will be no molecular weight dependence (Kolthoff and Gutmacher 1952, Chibowski 1990). Since the charge densities of the cationic starched are different, the dependency on the molecular weight is not detected. Less of the highly charged polymer is adsorbed at low ionic strength, as shown in Table 5.1.

If polyelectrolyte adsorbs in a more coiled conformation with loops and tails pointing out to the solution phase, the adsorbed amount is directly proportional to the molecular weight. Increase in molecular weight increases the adsorbed amount on smooth surface (Kolthoff and Gutmacher 1952, Chibowski 1990). Electrostatic interactions between cationic starch molecules and anionic silica surface are still valid although the NaCl concentration exceeds 100 mM since differences in adsorbed amount are still detected as seen in Figure 5.2. The attempt was made to examine the effect of molecular weight on adsorption using low charge density starch in 500 mM NaCl and high charge density starch in 100 mM NaCl in order to achieve more or less similar kind of polymer conformation.

Comparison of the adsorption of starches with low and high charge density at high ionic strength (100 and 500 mM NaCl) shows that more is adsorbed when the starch higher molecular weight is used. Furthermore, if curves I_a and II_b are compared (starch with low DS and high *Mw* in 100 mM and starch with high DS and low *Mw* in 500 mM), it can be seen that the $\Delta D/\Delta f$ –value at the end of the adsorption for both polymers under these conditions is ~36, which indicates layers with similar structure and properties. The final changes in frequency for starch with high *Mw* (DS=0.2) in 100 mM NaCl and for starch with low *Mw* (DS=0.75) are ca. -100 Hz and ca. -70 Hz respectively. Thus, the adsorbed amount increases with increasing molecular weight but other properties of the adsorbed layer are not significantly affected by the size of the molecule. However the interpretation of this experiment is difficult and somewhat speculative since the charge density is varying with molecular weight and the differences between these two effects can not be totally distinguished by these experiments.

The effect of polydispersity. Two starch samples with the following properties were investigated in order to clarify the effect polydispersity on the adsorption behavior: 1) starch with the *Mw* of 4.5×10^5 Da with clear unimodal molecular weight distribution and 2) starch with the *Mw* of 8.7×10^5 Da with a very broad distribution. For details, see Figure 1 in Paper I. Both starches have the same charge; the degree of substitution is reported to be 0.75 and the charge density is 1.5 meq/g.

Unpredictably, less of the high *Mw* starch is adsorbed and the same trend is observed regardless of the ionic strength, see Table 3 in Paper I and Figure 5.3. XPS fully supported the observation, see Figure 9 in Paper I. Viscoelastic properties were estimated by Voigt model in order to further explain the trend and the results are summarized in Table 5.3.

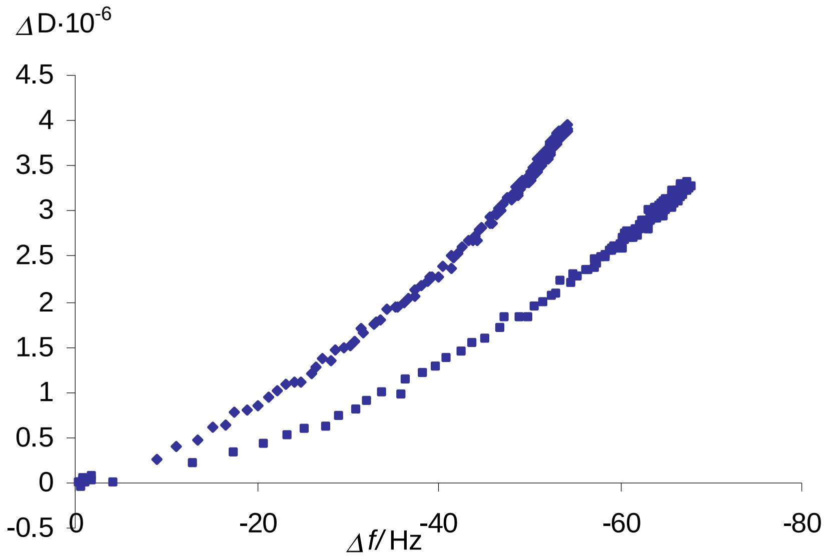

Figure 5.3. Change in dissipation factor as a function of the change in frequency for adsorption of 10 ppm CS with high degree of substitution in 100 mM NaCl. Key: (u) $Mw = 8.70{\cdot}10^5$ Da, (n) $Mw = 4.50{\cdot}10^5$ Da. $f_o = 5$ MHz, n=3.

In diffusion controlled adsorption the smaller molecules migrate to the surface faster than larger ones due to the smaller friction between the polyelectrolyte molecules and solvent molecules (Dukhin et al. 1995, Stenius 2000). Comparison of these two starches shows that less of the high molecular weight starch with broad distribution is adsorbed than of the low molecular weight starch with narrow distribution. The same trend is observed regardless of the ionic strength, Table 3 in Paper I and Figure 5.3. XPS analysis fully supports this conclusion, see Figure 9 in Paper I. Table 5.3 summarizes the effect of molecular weight and molecular weight distribution on the starch adsorption and on the viscoelastic properties of the formed layer. Figure 5.4 schematically illustrates the structure of the adsorbed layers.

Table 5.3. Summary of the effects of molecular weight distribution of cationic starch on adsorption and viscoelastic properties of the formed film.

	M_w= 4.5×10^5 Da, DS=0.75 narrow distribution	M_w= 8.8×10^5 Da, DS=0.75 broad distribution
$\Delta D/\Delta f$ (10 ppm solution)	48.0	72.3
C-O / %	9.8 ± 0.9	7.0 ± 1.6
N / %	0.86 ± 0.09	0.6 ± 0.2
η_f / Nsm^{-2}	(1.6 ± 0.1)·10^{-3}	(1.10 ± 0.03)·10^{-3}
μ_f / Nm^{-2}	(160 ± 30)·10^3	(94 ± 6)·10^3
τ_f/ns[1)]	9.2/10	12/13
h_f / nm	5.1 ± 0.1	4.8 ± 0.4

1) relaxation times calculated for adsorption at 20 min/90 min, see table 4 in Paper I.

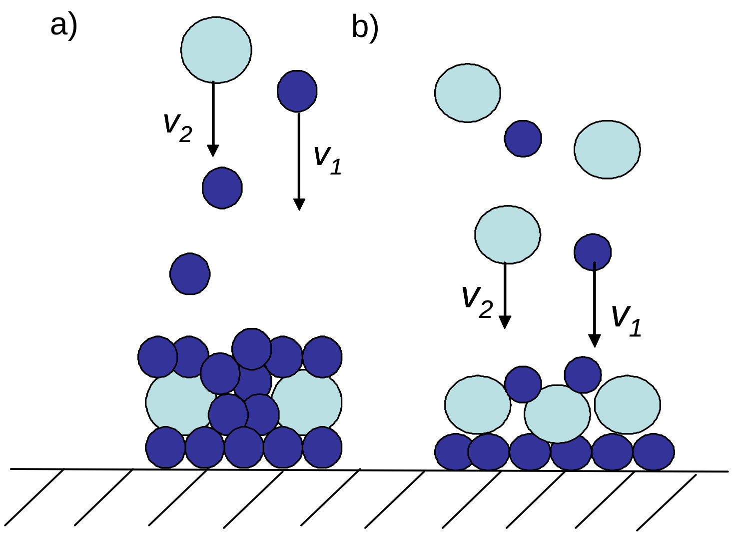

Figure 5.4. Schematic drawing of the structure of the layer of a) CS with narrow molecular weight distribution b) CS with broad molecular weight distribution. v_1 and v_2 represent the diffusion rates of the molecules of different size (v_1>v_2)

It is clearly seen from Table 5.3 that starch which has a narrow distribution of molecular weight forms a more compact and rigid layer (lower $\Delta D/\Delta f$, higher η_f and μ_f) due to the better packing of the starch molecules than the broadly distributed starch. The hydrodynamic thicknesses of the two layers do not differ much.

5.2 Model surfaces for the QCD-D adsorption studies (Papers II and III)

As shown by the results in the previous paragraph, the QCM-D technique is an excellent technique to perform the adsorption studies using papermaking chemicals and the results are well in accordance with the polyelectrolyte adsorption theories. Moreover, all the results (QCM-D data, QTools modelings and XPS results) were repeatable. The following step was to develop substrate surfaces, which better model the real main fiber components. Hence, in order to investigate the surface interactions in the TMP process waters, the model surfaces for cellulose, lignin and wood extractives were prepared. In this way the affinities of both papermaking chemicals and the dissolved and colloidal components originating from pulp on the fibrous material can be systematically studied.

5.2.1. Preparation of the model surfaces

Cellulose surface. Cellulose model films have been developed and investigated for years and the very recent review article covers the preparation, characterization and the use of cellulose model surfaces in the papermaking applications (Kontturi et al. 2006). In this work the application of Langmuir-Blodgett technique was used to deposit the trimethylsilyl cellulose (TMSC) on the polystyrene coated hydrophobic QCM-D crystal by using the horizontal dipping procedure (Figure 4.4). This technique is also often called as Langmuir-Schaefer (LS) method (Langmuir and Schaefer 1938). The dipping procedure is a slight modification to the procedure of Holmberg et al. (1997) who used the vertical procedure to prepare TMSC films on mica surfaces. The dipping parameters are given in Paper II. It was essential to use the horizontal procedure, because if the vertical procedure were used, the electrodes of the QCM-D crystal would have been contaminated.

The advantage of the LB- and LS-methods is definitely the possibility to control and follow the film transferring during the deposition by measuring the transfer ratio which is explained in the experimental section (Chapter 4.2.2). It was noticed that transfer ratios were more or less optimal and no detachment of the film was observed. Theoretically, a bilayer is formed during every dipping cycle (Lee et al. 1992) but stiff cellulose does not form a dense monolayer on the water surface. As a consequence, more dipping cycles are needed, in this case 15, to form a fully covering TMSC film. 15 dipping cycles lead to about 30 layers of TMSC on the QCM-D crystal surface. TMSC was regenerated back to cellulose by acid hydrolysis prior to the use in the adsorption experiments (Schaub et al. 1993).

Lignin and wood extractive surfaces. To my knowledge, the model films of spruce milled wood lignin and wood extractives from thermomechanical pulp have not previously been prepared. Model surfaces of Honduran pine lignin (Oliveira et al 1994), sugar cane bagasse lignin (Constantino et al. 1996, Pasquini et al. 2005), wheat straw lignin, wild cherry wood lignin (Aguié-Béghin et al. 2002) and kraft lignin (Norgren et al. 2006) have been prepared. The preparation technique used has been the Langmuir-Blodgett technique except Norgren et al. (2006) have used spincoating.

Since the solubility of milled wood lignin is very limited to all of the easily evaporating organic solvents, the LB-technique is very difficult to apply for preparing lignin films from MWL. Hence, the spincoating technique was chosen.

The Langmuir-Blodgett film deposition technique to prepare fatty acid layers has been known for decades (Langmuir 1917, Blodgett 1935, Petty 1996). However, the spincoating method was chosen for preparing extractive model surfaces due to the diverse composition of the TMP extractive mixture. This assured that all the wood extractive components were present in the right quantities. The MWL lignin and TMP extractive films were spincoated on the polystyrene coated QCM-D crystals. The spincoating recipes are given in Paper III.

5.2.2 Characterization of the model surfaces

The morphology, coverage and chemical composition of the model surfaces were characterized using AFM and XPS. Stability studies of each type of the model film, when used in the adsorption experiments, were conducted by using QCM-D.

Morphology and thickness of the model surfaces. Figure 5.5 shows the AFM topography images of polystyrene, TMSC after 15 dipping cycles and cellulose surface after 3 and 15 dipping cycles. After 15 deposition cycles of TMSC, the structure of the surface clearly changes, as can be seen from Figure 5.5b. After three deposition cycles the crystal surface was not fully covered by cellulose (Figure 5.5c) and it contained holes. After 15 deposition cycles only the cellulose structure is seen, Figure 5.5d. A smooth and thin cellulose surface was achieved with rms roughness of approximately 0.4 nm determined from a 1μm x 1 μm topography image. The TMSC film is rougher (rms roughness of 0.8 nm) than the cellulose, because the three methyl silyl groups are much larger than one hydroxyl group. The transformation from both, a rough TMSC film and an open cellulose film to finally a smooth and homogeneous cellulose film is clearly visible when comparing the line profiles of the images in Figures 5.5 b-d. The final thickness of the cellulose film, estimated using the Nanoscope image processing depth profiling tool, was calculated to be 11.5 nm, which is in good accordance with Holmberg et al. (1997).

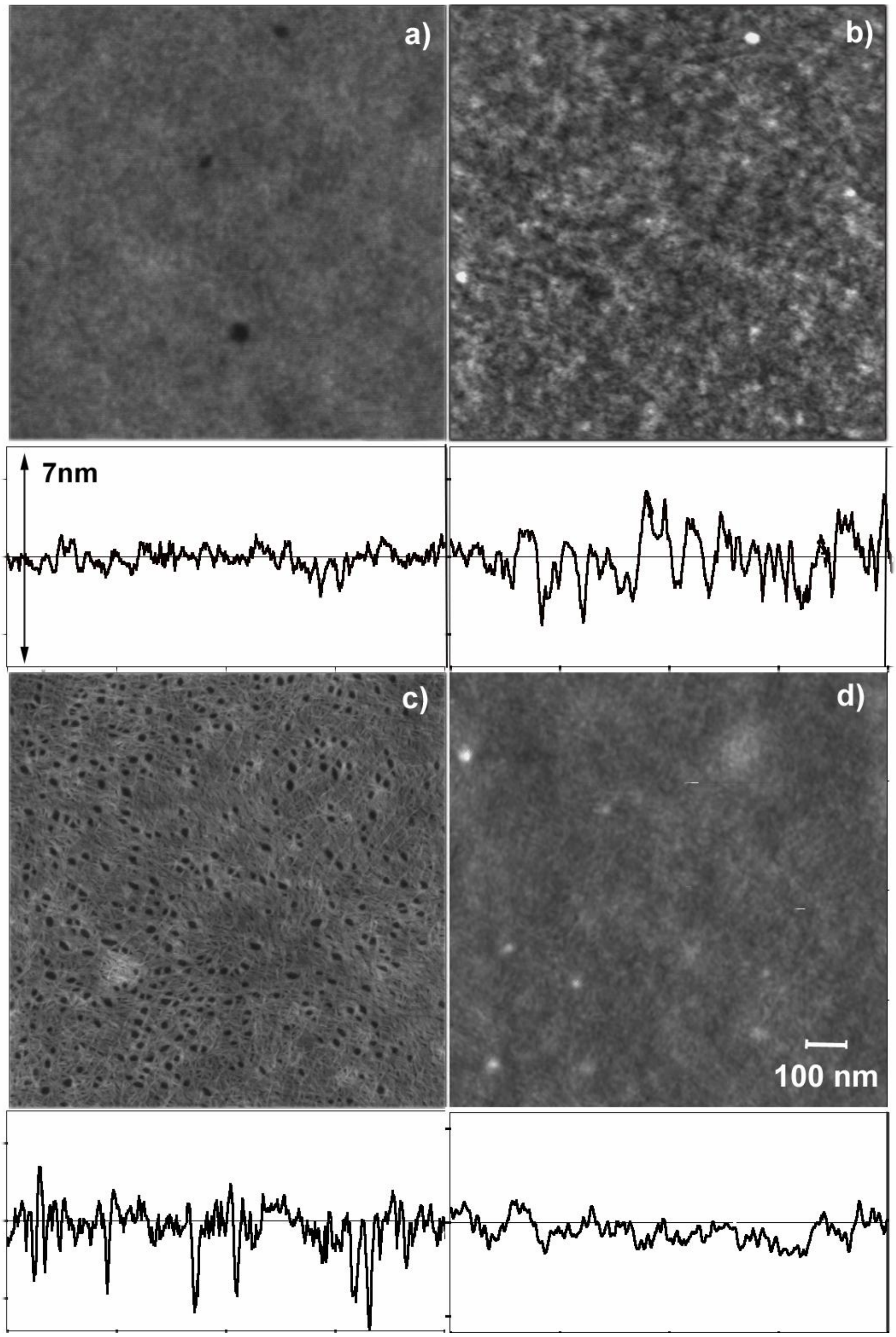

Figure 5.5. AFM topography images of a) polystyrene, b) TMSC after 15 dipping cycles and cellulose after c) 3 and d) 15 dipping cycles. Height profiles of the surfaces are also shown. The image size is 1 μm^2.

Figure 5.6 shows AFM topography and phase contrast images of a pure polystyrene surface on the QCM-D crystal (a and d) as well as of films of milled wood lignin (b and e) and TMP extractive mixture (c and f) spincoated on the polystyrene. Lignin and extractive films fully covered the crystal surface and they were moderately smooth. The rms roughness of polystyrene, lignin and extractive surface was approximately 0.3 nm, 0.4 nm and 1.1 nm, respectively, determined from the 1 μm x 1μm AFM topography images. The extractive surface was not chemically as homogenous as the lignin surface (differences detected in phase image, see images e and f) and the surface topography was slightly rougher. This is probably due to the different extractive components (fatty and resin acids, triglycerides and sterols, see Table 4.1) present in the TMP resin mixture. Due to the sticky nature of the extractive film, those surfaces were difficult to image and some noise is seen in the topography and phase contrast images (images c and f). However, the surface was fully covered with the resin. The height profile determinations gave also a coarse estimation of the lignin and wood extractive film thicknesses. The final thickness of the lignin film varied between 200 and 300 nm, whereas TMP extractive mixture coatings yielded in the thickness values of 80-150 nm.

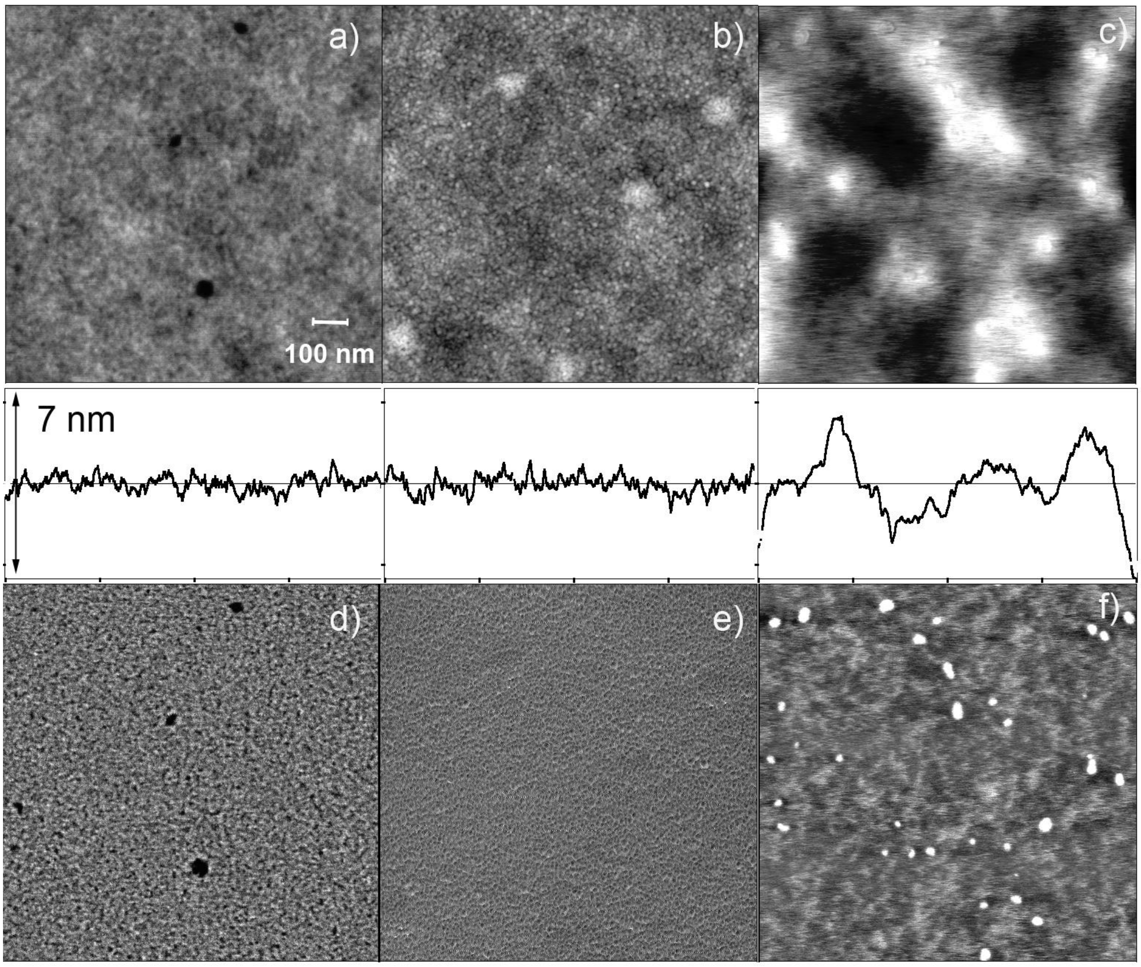

Figure 5.6. AFM topography images of a) pure polystyrene, b) spincoated MWL lignin and c) spincoated TMP extractive mixture and phase contrast images of d) pure polystyrene, e) spincoated MWL lignin and f) spincoated TMP extractive mixture on polystyrene surface in air. Typical height profiles are shown in the middle. The image size is 1 μm^2.

*Chemical composition of the model surfaces***.** Identification of polystyrene, cellulose, lignin and extractive films deposited on the QCM-D crystal was based on the XPS analysis using the relative abundance of C-C carbon, i.e. unoxidized carbon and the oxygen/carbon (O/C) atomic ratio. They are the characteristic quantities for each of the components studied (Gray 1978). Pure cellulose contains no unoxidized carbon, whereas pure polystyrene consist only of C-C carbon with no oxygen present in its chemical structure. In theory, the O/C ratio is 0.83 for pure cellulose and 0 for pure polystyrene. Theoretical values of O/C ratio for lignin and oleic acid (fatty acid in resin mixture) are 0.33 and 0.11, respectively. Theoretically, the relative abundance of C-C carbon is 49 % for lignin and 94% for oleic acid. By comparing the theoretical and measured values, it is possible to verify how successful the film deposition was (Johansson et al. 2005).

Theoretical and measured values for each component are shown in Figure 5.7. They are very well in accordance with each other. For both MWL and polystyrene the theoretical and measured values are very similar. The values for the TMP resin film are also close to the values for pure oleic acid. The slight difference observed is due to the fact that the extractive mixture contains also other extractive components than oleic acid.

The largest difference in theoretical and measured values was in the case of the cellulose model film. Pure cellulose has no C-C component of the C1s signal but cellulose model film gives quite high percentage of these particular bonds. It is very likely that these bonds detected from cellulose coated crystal origin from the underlying polystyrene. The thickness of the cellulose film was estimated to be approximately 11.5 nm. Since the cellulose film was porous the XPS analysis depth may be higher although the analysis depth for polymeric material is 6-12 nm (Ashley and Williams 1980). After 30 depositions the cellulose film was probably so thin that XPS still detects the underlying polystyrene. However, full coverage of the cellulose film was observed by AFM (Figure 5.5d) and IR results support acceptable quality of the cellulose (see Figure 2 in Paper II).

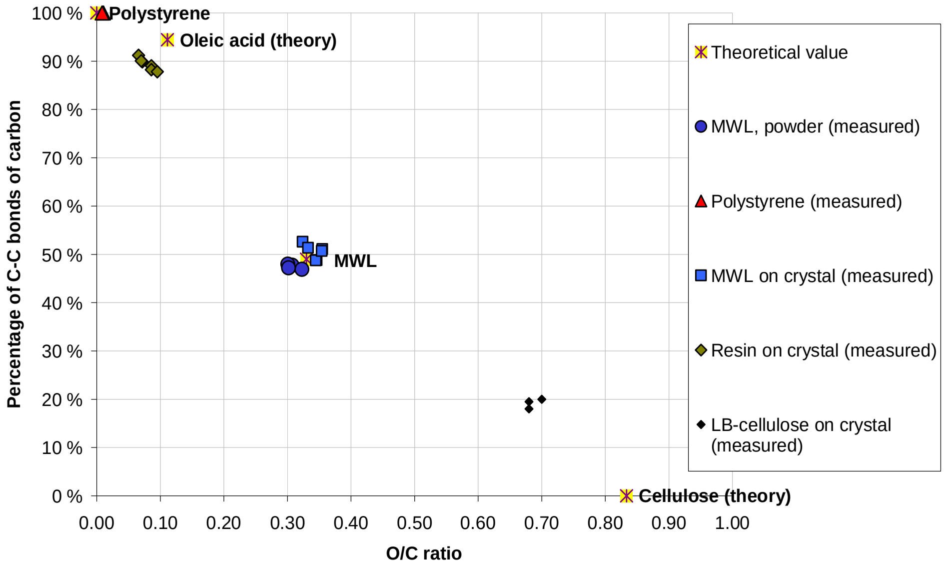

Figure 5.7. Theoretical and measured values of relative abundance of C-C bonds as a function of the oxygen/carbon ratio for polystyrene, extractives, lignin and cellulose.

Stability of the model surfaces. In dilute aqueous solutions polyelectrolyte molecules swell due to the osmotic pressure created by the counter-ions. Swelling of the polyelectrolyte film can be a very slow process and it depends on the solution pH and electrolyte concentration. (Flory 1953) Hence, the swelling and the stability of all the model films were investigated with QCM-D.

Figure 5.8 shows an example of the behavior cellulose model film deposited on polystyrene at sequentially increased ionic strength. In QCM-D stability studies a decrease in frequency is thought to indicate water penetration into the layer structure and/or possible swelling. Changes in dissipation describe changes in structural properties such as layer softening and thickening during these processes. A higher dissipation response corresponds to softer layers. From Figure 5.8 it is clear that water penetrates into the cellulose film because the frequency decreases. The small positive change in dissipation indicates that slight swelling of faintly negatively charged cellulose film occurs. Yet, no considerable layer softening occurred and the film stays rigid ($\Delta D < 0.5 \cdot 10^{-6}$). When the electrolyte concentration was slightly increased (1 and 10 mM NaCl) the change in dissipation of the cellulose film decreases. Hence, there seems to be some decrease in swelling. Such deswelling was not seen with polystyrene due to the negligible charge of the film. After electrolyte addition the dissipation change remained more or less constant for polystyrene (Figure 9 in Paper II). The cellulose film was regarded as fully swelled and stabilized after 6 hours in contact with deionized water.

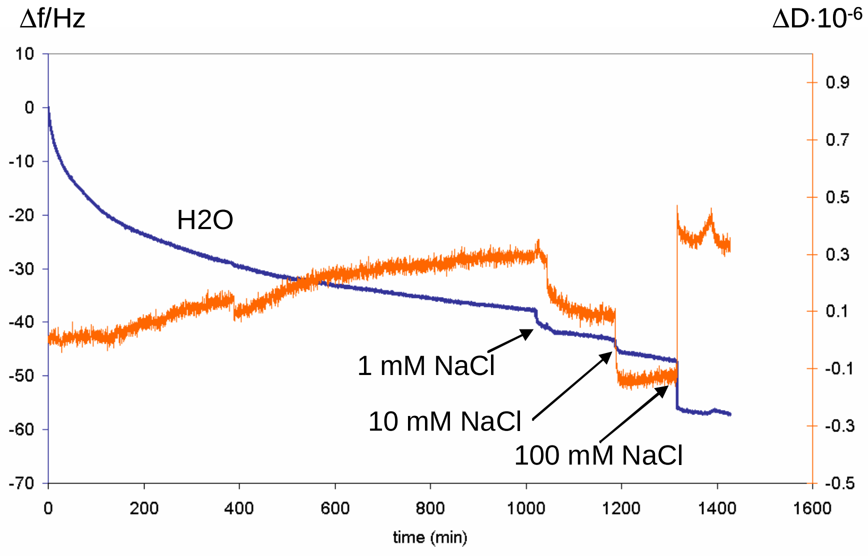

Figure 5.8. Change in frequency and dissipation as a function of time during the swelling and stabilation of cellulose model film in water/aqueous electrolyte solutions with increasing ionic strength. Electrolyte concentration increases sequentially. f_0=5 MHz, n=3.

Some amount of water/electrolyte solutions also penetrated into the lignin structure, but no positive change in dissipation was detected during the experiments, indicating that no layer softening was taking place. Thus, the MWL lignin films do not swell in aqueous solution (Paper III). The lignin film was fully stabilized after 5 hours in contact with deionized water.

Solubility and the saponification of the fatty and resin acids in basic conditions limit the usable pH range of the TMP extractive surface. Hence, TMP extractive surfaces have a very pH dependent character. The TMP extractive model surface was stabilized almost immediately after the immersion of the crystal surface into the water when the pH was kept neutral or acidic. Figure 5.9a shows that after addition of water (pH 7.5 and pH 5), the changes of frequency and dissipation remained constant. The peaks at time 40 min were due to the severe solution addition on the crystal surface (liquid peak). The pK_a values of acids present in TMP extractive mixture vary between 5.0 and 6.4 (Ström, G. 2000, p.140), meaning that they are insoluble in water only in acidic conditions. It was found that the extractive films are also stable at higher pH (pH 7-8) probably due to the neutral components (sterols) present in the resin mixture. Neutral components have been shown to decrease the water solubility of the fatty and resin acid mixtures (Pirttinen et al. (2004)).

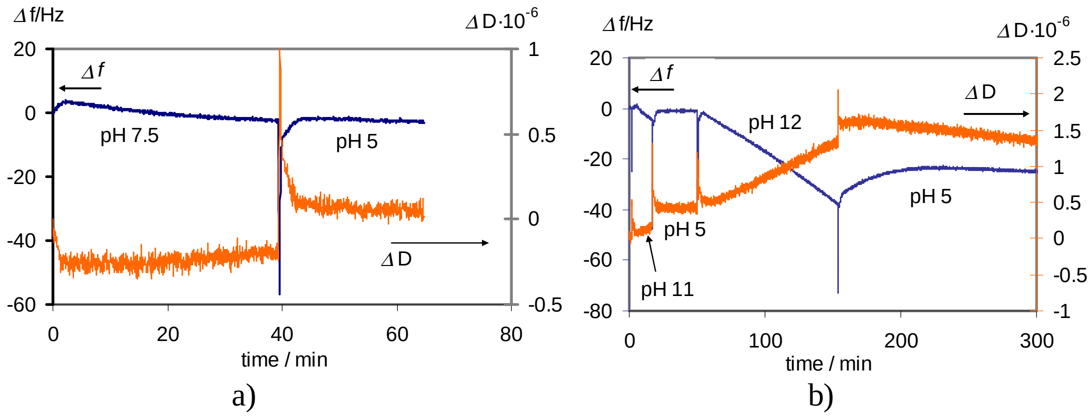

Figure 5.9. Change in frequency and dissipation as a function of time during the stabilization of the spincoated TMP extractive film at different pH. f_0=5 MHz, n=3.

In acidic form the fatty and resin acids are stable and insoluble in water but in basic conditions the acids saponify, form liquid crystal structures and, as a consequence, the model film is no longer stable. When in contact with a basic solution the film was very unstable, as seen in the Figure 5.9b. When the pH was adjusted to basic conditions the frequency started to decrease rapidly with a concomitant increase in the dissipation factor. This indicates an increase in the mass attached to the crystal and that the extractive layer becomes softer. The detected mass change is apparently due to changes in the extractive layer structure, i.e. the layer becomes able to bind more water. Extractive layer containing resin and fatty acids starts to swell as the carboxylic groups begin to ionize. When the pH is increased, the saponification of the fatty and resin acids starts and the layer structure probably reorganizes forming a lamellar liquid crystal-like structure with water between the bilayers. Extensive swelling of the lamellar phase with bilayers of acids and soaps with water is a well-known phenomenon (*e.g.* Jönsson et al. 1998; Stenius et al.1984). The information received with QCM-D gives no direct answer to the structural changes, and other techniques such as SAXS or AFM could be used to further clarify the layer structure and its pH dependency on the TMP extractive model film.

5.3 Adsorption of dissolved hemicelluloses and wood extractive colloids on model surfaces (Papers IV and V)

The aim of the last part of this work was to better understand on a molecular level the interactions present in the wet end of the paper machine when dissolved and colloidal substances are present together with fibrous material. The goal of the study was to clarify how e.g. peroxide bleaching and increased ionic strength change the interactions between dissolved hemicelluloses, colloidal extractives and different fiber components. Model surfaces which represent fibrous material (cellulose, lignin and wood extractives) were used to study the adsorptions of dissolved hemicelluloses and colloidal extractives separately on each surface. Moreover, few observations of practical experiments are explained by these fundamental surface chemistry findings.

5.3.1 Adsorption of dissolved hemicelluloses

Adsorption of dissolved hemicelluloses isolated from unbleached and peroxide bleached thermomechanical pulp on cellulose, lignin and wood extractive surfaces are primarily discussed with respect to the effect of electrostatic interaction on the affinities between hemicelluloses and substrate surfaces. The composition of the hemicellulose fractions are shown in Table 4.3.

The charge density of the cellulose surface is anionic but very low. The lignin surface can be regarded to be neutral and the wood extractive surface has an anionic charge due to the dissociated carboxyl groups of fatty and resin acids.

On the basis of the charge determinations of the hemicelluloses, the fractions of dissolved hemicelluloses could be regarded as mixtures of anionic polyelectrolytes with different size distributions and charge densities. Dissolved hemicellulose fraction isolated from unbleached TMP mainly consisted of neutral O-acetyl-galactoglucomannans. The contributors to the anionic charge of this fraction are arabinogalactans and pectins. These hemicelluloses, especially pectins, are present only in minor amounts in this hemicellulose fraction. Thus, the fraction of hemicelluloses isolated from unbleached TMP has a moderately low charge density, 0.51 meq/g. Although the size distribution of the fraction is not defined, it is known that the fraction is a mixture of small molecular weight components (pectins) and dominating larger polymeric material (galactoglucomannans and arabinogalactans) (Thornton et al. 1994).

The fraction of hemicelluloses isolated from peroxide bleached TMP can be referred to a moderately highly charged polyelectrolyte mixture. The charge density of the fraction was 1.38 meq/g. Increasing content of pectic material with concomitant decrease of galactoglucomannan content increases the net charge anionic charge of the mixture. It can be assumed that the size distribution is changed so that smaller polymeric molecules are present to a larger extent. Pure galactoglucomannan and pure pectin samples showed the unimodal molecular weight distribution, analysed by SEC in Åbo Akademi. Pure galactoglucomannan is rather large neutral polymer, whereas pure pectin is a small and highly charged anionic polyelectrolyte.

*The effect of ionic strength and substrate***.** Figure 5.10 compares the adsorption experiments of dissolved hemicelluloses isolated from unbleached TMP performed on cellulose, lignin and extractive model surfaces at low and high ionic strength.

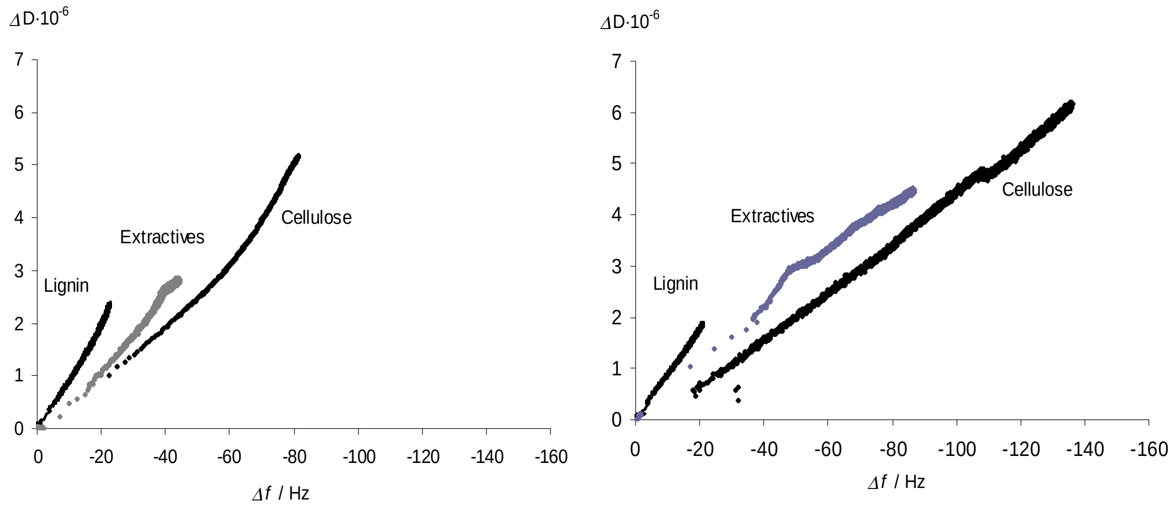

a) b)

Figure 5.10. Change in dissipation as a function of the change in frequency for adsorption of 100 ppm hemicellulose solution on cellulose, lignin and extractive surfaces. (a) 0 mM NaCl and (b) 100 mM NaCl. Hemicelluloses are isolated from unbleached TMP. 10 mM NaAc/HAc buffer, pH 5.6. f_0 = 5 MHz, n = 3, t = 200 min.

Comparison of Figures 5.10a and b shows that the change in both frequency and dissipation was higher for adsorption from 100 mM NaCl solutions than for pure buffer solution, especially when cellulose and extractive surfaces were used as substrates. Due to electrostatic interactions, adsorption of dissolved hemicelluloses is expected to increase with increasing ionic strength for two reasons. First, repulsion between the anionic surface and the anionic dissolved hemicellulose components is effectively screened. Secondly, the charged hemicellulose chains can adopt a more compact conformation. Adsorption of dissolved hemicelluloses on the lignin surface was not significantly changed by the increased electrolyte concentration.

Hemicellulose adsorption on cellulose surface can be considered as adsorption of an anionic or neutral polyelectrolyte on a very weakly anionic surface. The repulsion between like charges (polyelectrolyte-surface) is so low that other attractive interactions predominate and significant amounts of hemicelluloses attach to the cellulose surface, Figure 5.10a. Increasing the ionic strength lowers the repulsion between the anionic segments of the hemicellulose, resulting in a more coiled conformation of the polyelectrolyte chain. As a consequence, more polymer can fit onto the surface (Figure 5.10b). These effects are the similar but more pronounced when extractive surface is used due to the higher anionic charge density of the surface.

The results do not indicate any specific tendency of the hemicelluloses to adsorb on the lignin surface. The reason for the weak hemicellulose adsorption on lignin might be just that polymers tend to go to surfaces instead of being in the solvent. Probably in the process waters where the high mechanical stress affect and other more attractive surfaces are present for hemicelluloses to adsorb, they do not adsorb on lignin at all or at least if adsorbed they would easily desorb.

The effect of peroxide bleaching. Neutral galactoglucomannan is a major compound in a hemicellulose fraction isolated from unbleached TMP pulp. Due to the deacetylation of galactoglucomannans in peroxide bleaching stage, they tend to sorb back to the fibre surface and their amount decreases significantly in water phase (Holmbom et al. 1991, Thornton et al. 1994). Release of highly anionic pectic material from the fibers occurs simultaneously. As a consequence, the hemicellulose fraction contains more small, highly anionic pectin acids after peroxide bleaching. In order to obtain a better understanding of hemicellulose adsorption and the effect of bleaching (the effect of increased charge density of the polyelectrolyte), the major/predominant components of each hemicellulose in the mixture of unbleached or bleached fraction were adsorbed separately on each model surface.

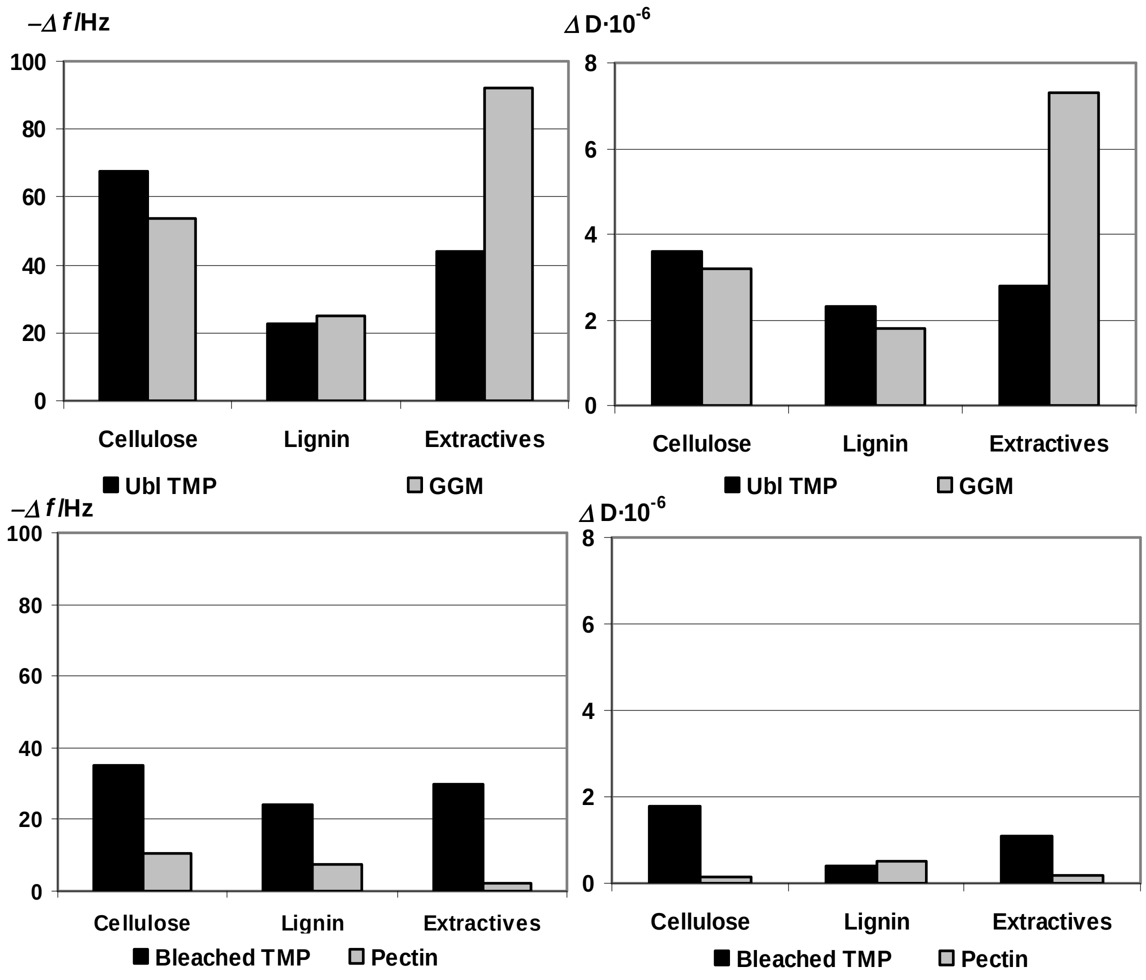

Figure 5.11. The final changes in frequency and dissipation for adsorption of 100 mg/l unbleached hemicellulose fraction (Ubl TMP), O-acetyl-galactoglucomannan (GGM), peroxide bleached hemicellulose fraction (Bleached TMP) and pectin ppm on cellulose, lignin and extractive surfaces. 10 mM NaAc/HAc buffer, pH 5.6. f_0 = 5 MHz, n = 3, t = 100 min.

Figure 5.11 compares the final changes in frequency and dissipation for the adsorptions of unbleached hemicellulose fraction and pure galactoglucomannan solution as well as the peroxide bleached hemicellulose fraction and pure pectin solution on cellulose, lignin and wood extractive surfaces.

The adsorption behavior of unbleached hemicellulose fraction and pure galactoglucomannan resembles very much each other. On cellulose the adsorbed amount is significant whereas on lignin the adsorbed amount is notably smaller. The results are in good accordance with the observations of Hannuksela et al. (2003). They found that galactoglucomannans did not sorb on lignin covered TMP fibers but, on the contrary they extensively sorbed on cellulose rich kraft fibers.

Large amounts of pure galactoglucomannan adsorbed on extractives, which indicates that galactoglucomannans play a major role in creating steric hindrance around colloidal extractives. These results show clearly why the hemicelluloses isolated from unbleached TMP can effectively sterically stabilize extractive colloids. The hemicelluloses, indeed, adsorb extensively on the extractives and on cellulose forming a layer with loops and tails pointing out the solution phase. The observation supports the findings in the work of Hannuksela et al. (2004a) who showed that especially the mannan affects the stabilizing ability rather than galactose side groups. The dependence on ionic strengh is in good accordance with the polyelectrolyte adsorption theories (Fleer et al. 1993) but the nature of the main driving force of adsorption, which definitely is not electrostatic, is still uncertain. On cellulose surface the hemicelluloses probably adsorb due the similarities in the molecular structure which could promote the formation of hydrogen bonds in analogy with those between cellulose chains in crystalline cellulose. The adsorption is more pronounced when the repulsion between like charges is screened.

As expected, much less of the dissolved hemicelluloses isolated from peroxide bleached TMP is adsorbed on each surface, see Figure 5.11. The repulsion between charged carboxylic acid segments of the hemicellulose chain is high, leading to a stiff, rod-like conformation of the polyelectrolyte molecules. Thus, hemicelluloses isolated from peroxide bleached TMP should tend to form a flat layer when adsorbed on wood components. Adsorption behavior of pure pectin supports this idea. The low M_w, highly charged pectin adsorbed on cellulose and on lignin forming a very thin and flat layer. At low ionic strength the high repulsion between the extractive surface and pectin more or less prevented adsorption.

5.3.2 Adsorption of extractive colloids

Purely electrostatically stabilized colloidal extractives adsorbed to all surfaces but to the largest extent on the cellulose surface (Figure 5.12). This was not as expected, since both the colloid and the cellulose surface are negatively charged. Clearly, non-electrostatic interactions play an important role in this adsorption. The lowest amount of extractive colloids adsorbed on the extractive surface. This is explained by the high anionic charge of the extractives leading to a strong repulsion between the extractive surface and colloid. Increase in ionic strength does not lead to screened repulsion between the surface and colloids as expected, since colloids remain stable at this ionic strength. Thus, any kind of attraction towards the extractive surface is not detected at high ionic strength, see Figure 5.12b.

The increased adsorption to cellulose and lignin upon NaCl addition is explained by screening of repulsive anionic charges of the colloids. Although the colloids are still stable at this ionic strength (40 mM) and they do not precipitate, the stability of the colloids is decreased to some extent. The particle size and the size distribution were observed to slightly increase (results not shown). However, the size of the dispersion was within the size distribution of the colloidal material. This minor disruption of the colloidal stability seems to lead to higher adsorbed amounts of extractives on cellulose and on lignin probably due to slightly larger colloids (Figure 5.12b). Furthermore, when adding NaCl, the repulsive surface charges between the electrostatically stabilized anionic colloids and anionic cellulose surface are screened, allowing other surface interactions to become more prominent.

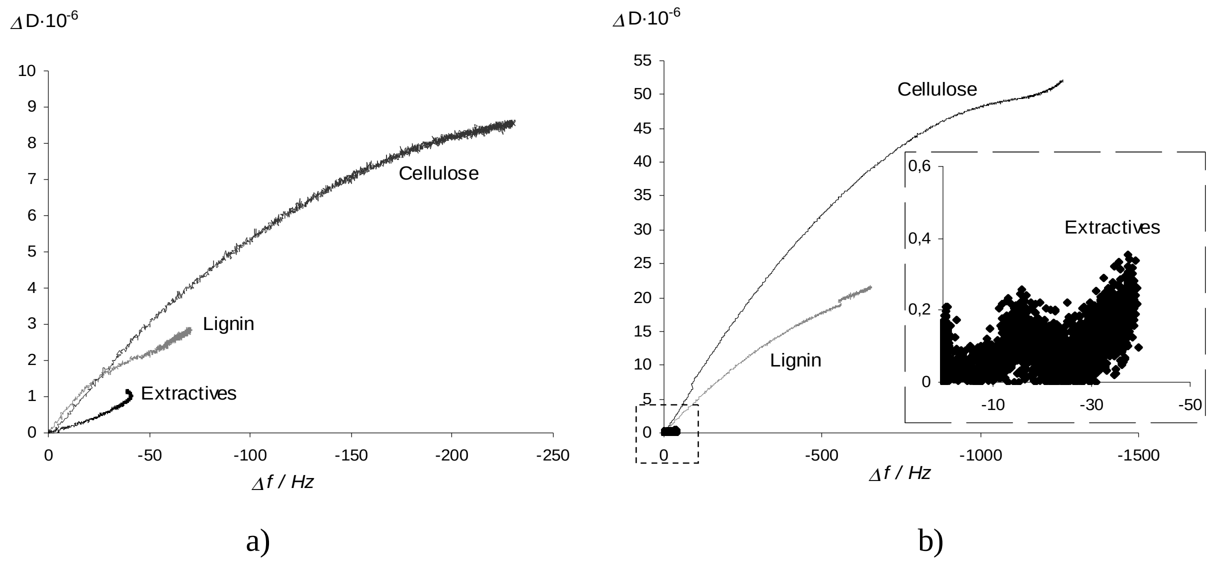

Figure 5.12. Change in dissipation as a function of the change in frequency for adsorption of 100 mg/L electrostatically stabilized colloidal extractives on cellulose, lignin and extractive surfaces. (a) 0 mM NaCl and (b) 30 mM NaCl. 10 mM NaAc/Hac buffer, pH 5.6. f_0 = 5 MHz, n=3, t =100 min. The excerpt shows an enlargement of the colloid adsorption on the extractive surface at high ionic strength.

The effect of dissolved hemicelluloses on the adsorption behavior of the colloidal material is discussed more thoroughly in the following paragraph. These results were used to illuminate some observations achieved when extractive colloids were selectively adsorbed on fines. Colloidal interactions in process waters, how they retain in the paper sheets and how they affect the paper surface properties are also briefly discussed by combining results achieved from QCM-D, AFM and sheet experiments.

5.3.3 Adsorption of extractive colloids on TMP fine material

During thermomechanical pulping the fines are created by peeling of the wood fibres (Luukko 1999). Fines enriched in flake-like material are produced in the 1st refining state and they come from the outer part of the cell wall and middle lamella which contains high amount of lignin and hemicelluloses. Mosbye et al. (2002) found that flake type of fines contained more pectic material than fibrillar fines which may explain the differences in total charge of the fine material (see Paper V, Figure 2). Total charge of the flake-like fines was higher than that of fibrillar fines. Mosbye et al. (2003) also found that cellulose content increased while lignin content decreased when the fines originated from further inside of the fibre wall (fibrillar type of fines after the 3rd refining state). Flake-like fines contain also more extractives than fibrillar fines. The chemical composition and other properties of the flake-like and fibrillar fines used in this work were well in accordance with the findings of the other research groups (Kleen et al. 2003, Luukko et al. 1999 and Mosbye et al. 2002 and 2003).

It was found in paper V as well as in the work conducted by Mosbye et al. (2003) that sterically stabilized colloidal wood resin adsorbed selectively to TMP flake-like fines. On the other hand, in the presence of purely fibrillar fines the colloids remained in the solution phase showing no affinity towards fibrils. Figure 5.13 shows the effect of steric stabilization by dissolved hemicelluloses isolated from unbleached TMP on the adsorption of colloidal resin to the different fines.

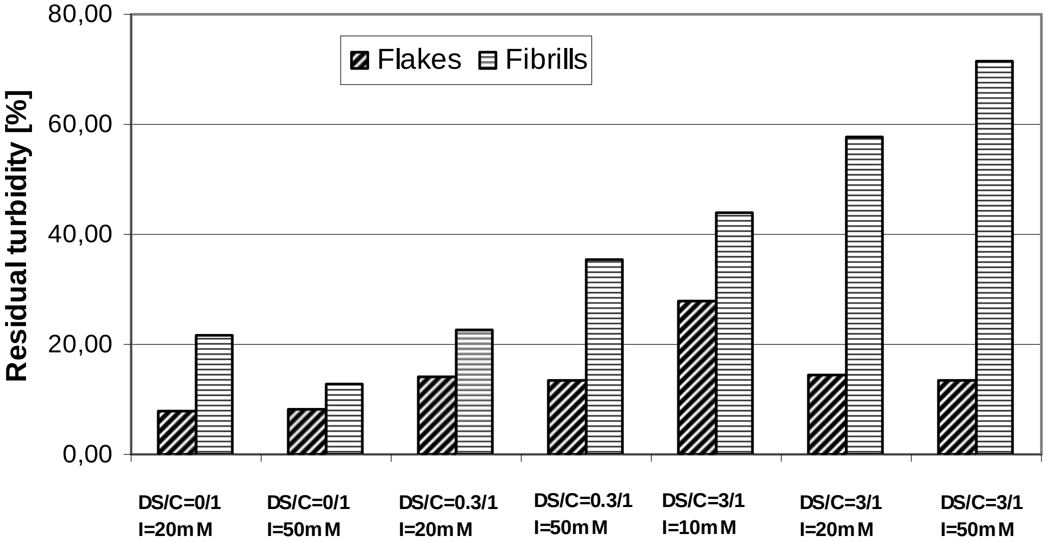

Figure 5.13. Turbidity due to residual wood resin after adsorption in the presence of fibrillar and flake-like fines in different chemical environments (ionic strength and dissolved substances). DS=dissolved substances, C=colloids.

The reason for the differences in colloidal adsorption is expected to appear due to the differences in the surface composition of the fines material. Two explanations were suggested to clarify the observation: 1) attractive hydrophobic interactions between extractive colloids and extractive and lignin rich flake-like fines and 2) steric hindrance created by hemicelluloses adsorbed on surfaces and on colloids, which prevents the colloids from adsorbing on fibrillar fines.

Paper IV gives some additional information to support or to disprove the hypotheses by means of hemicellulose and colloid adsorption studies. First, it was shown in Paper IV that if steric hindrance was created around the colloids and also on the adsorbent surface by preadsorbing hemicelluloses, the adsorption of colloids on any surface was more or less prevented, see Table 5.4. Attractive hydrophobic interactions between sterically stabilized colloids and extractive surface are not strong enough to overcome the hindrace between the hemicellulose layers. According to the QCM-D results there must be some uncovered surface left for extractive colloids to adsorb due to the fact that if the whole system is sterically stabilized, the colloid adsorption is more or less prevented regardless of the substrate surface, see Table 5.4.

Table 5.4. Δf for the adsorption of extractive colloids on different model surfaces at high ionic strength. f_0 = 5 MHz, n=3.

	Electrostatically stabilized colloids	Sterically stabilized colloids	Sterically stabilized system*
Cellulose	-1280	-303	-70
Lignin	-666	-144	-42
Extractives	-42	-99	-15

*Sterically stabilized colloids adsorbed on preadsorbed hemicellulose film.

The areas on the flake-like fines which might have been left uncovered when adsorbing the hemicelluloses could be the lignin rich areas. Some hemicelluloses adsorb on lignin surface, see Figure 5.10, but further investigation of the layer properties indicates that the hemicellulose film is not very strongly bound on lignin. When compared to the film formed on cellulose the hemicellulose film is more strongly bound. Both shear viscosity and shear elasticity values estimated using the Voigt-based model (modeling results are shown in Figure 5.14) are significantly lower for hemicellulose film adsorbed on lignin and the formed layer is notably thinner, indicating rather weakly bound film, see Figures 5.15 and 5.16. It can be assumed that in the presence of higher shear forces and other more attractive surfaces for hemicelluloses to adsorb, the hemicellulose film easily desorb if adsorbed in the first place. As a consequence, the sterically stabilized colloids probably adsorb on the lignin containing areas of the flake like fines which are not covered by hemicelluloses.

a)

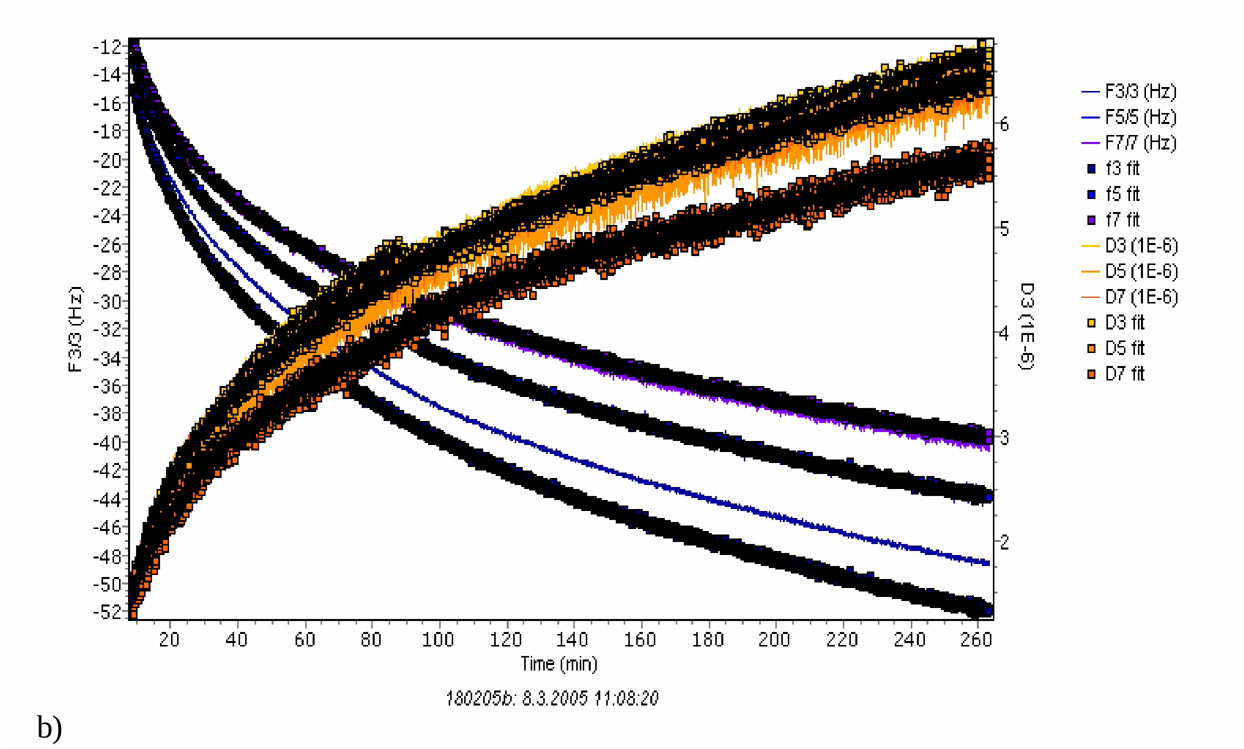

b)

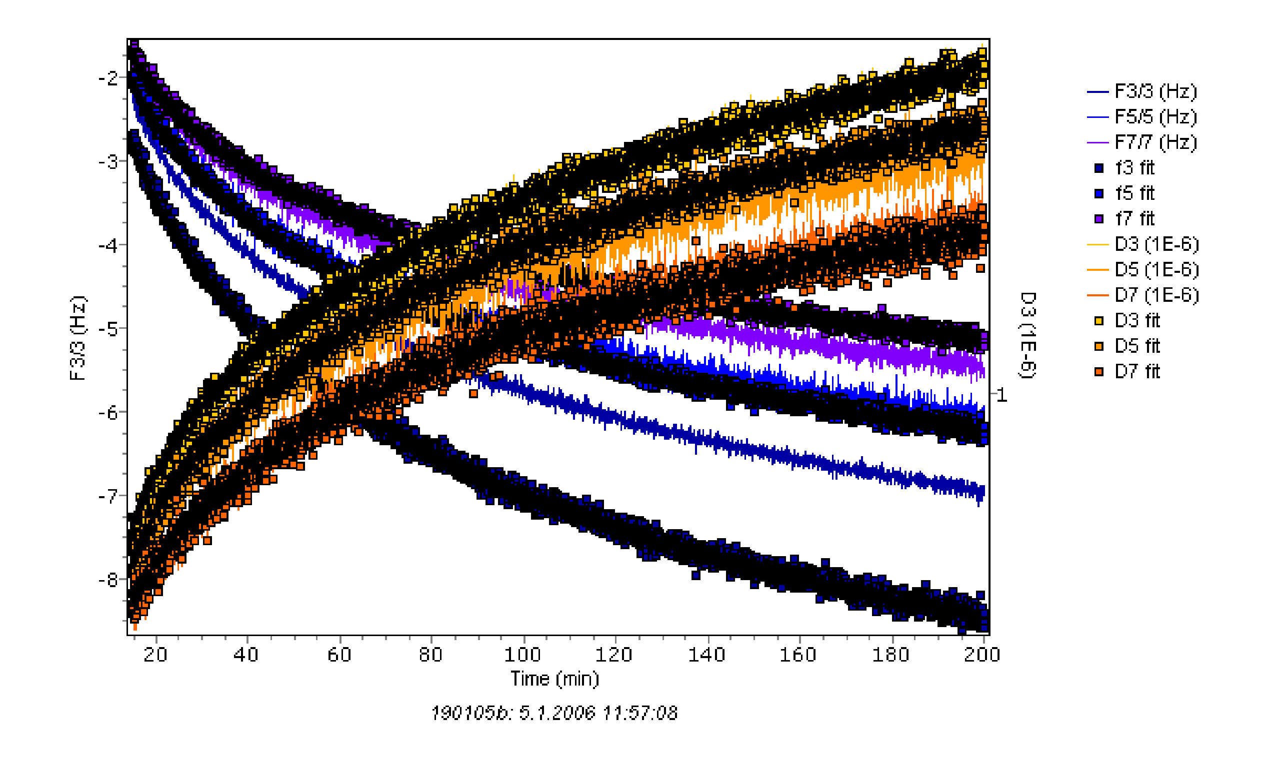

Figure 5.14. Adsorption of hemicellulose solution in 100 mM NaCl. Hemicelluloses were isolated from unbleached TMP. Δf and ΔD versus time at n = 3, n = 5 and n = 7 (lines indicate QCM-D data) and the best fit obtained using Voigt model (squares indicate fitted values). (a) cellulose surface (b) lignin surface. 10 mM NaAc/HAc buffer, pH 5.6. Assumed layer density = 1.2 g cm^{-3}. Tammelin et al. (2006).

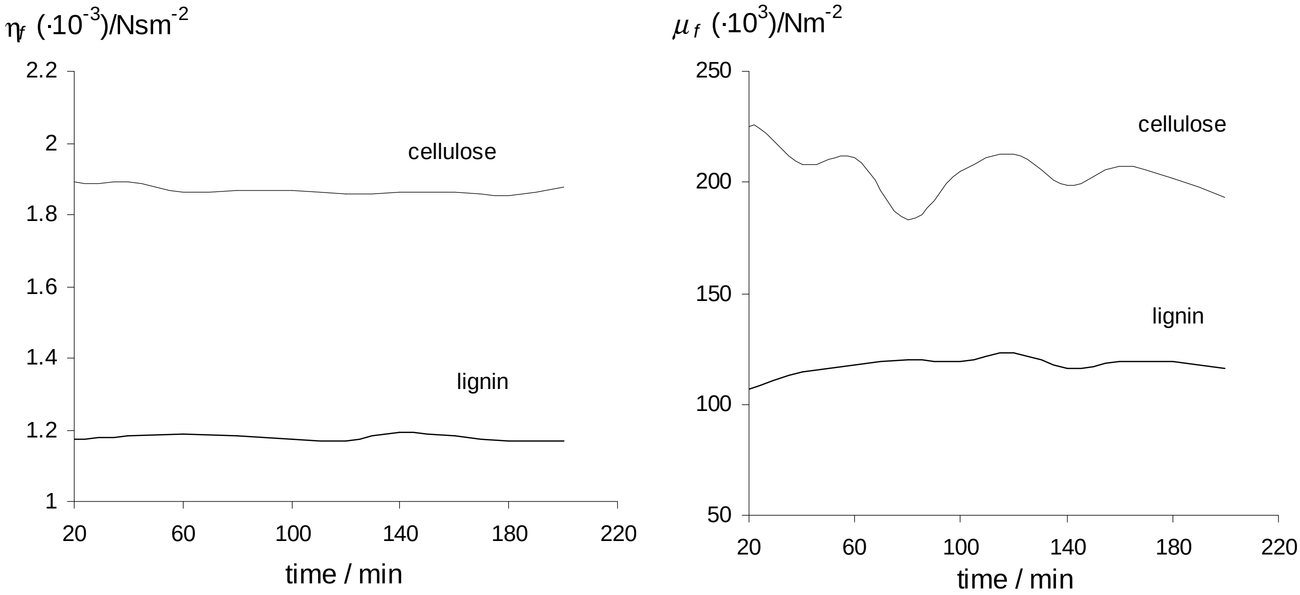

a) b)

Figure 5.15. Variations in a) the shear viscosity and b) shear modulus as a function of time corresponding to the best fit curves in Figures 14 a and b.

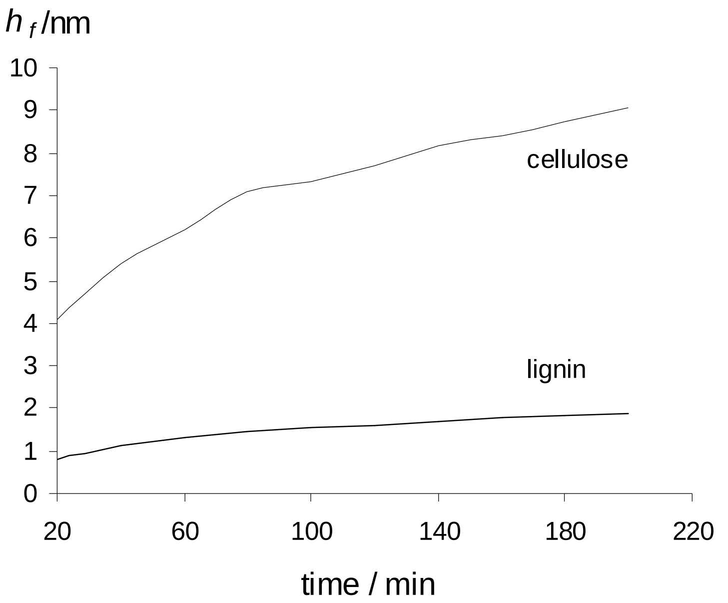

Figure 5.16. The hydrodynamic thickness of the hemicellulose film on cellulose and on lignin in 100 mM NaCl.

The fibrillar types of fines seem to be effectively covered by hemicelluloses. As shown by the QCM-D results in Paper IV, the decrease in adsorption of colloids due to steric hindrance is the most pronounced on cellulose, see Table 5.4. The frequency change detected on cellulose surface when extractive colloids were adsorbed decreases in the following way: -1280 Hz → -303 Hz → -70 Hz in the order of pure colloids, sterically stable colloids and sterically stable system. This supports results observed with fibrillar fines in Paper V. No turbidity reduction due to colloid adsorption in sterically stable colloidal suspension in the presence of fibrillar fines was observed (Figure 5.13).

5.3.4 Indentification of wood extractives on cellulose (New results)

On the basis of the previous AFM and XPS studies conducted by Koljonen et al. (2004) the wood extractives seem to spread as a thin film on paper surface. However, the interpretation of the AFM images of the different structures of the heterogeneous pulp samples is complex and additional techniques and model systems need to be used as the verification methods. Österberg et al. (2005) precipitated colloidal extractives on model cellulose surfaces and detected also the thin film formation of extractives. Fardim et al. (2005) used a combination of XPS, ToF-SIMS and AFM to study the single resin components on different pulps. They found that stearic acid and its calcium salts formed aggregates while oleic acid formed a uniform layer. In a very recent study by Österberg et al. (2006), a combination of confocal Raman spectroscopy and AFM was used to study the wood extractives on cellulose surfaces. For the first time, it was possible to obtain both morphological and chemical information from the same sample location, and important chemical evidence of the AFM phase shift images was achieved.

In order to further clarify the interpretation of the extractive morphology on cellulose surface, the cellulose coated QCM-D crystals were measured with AFM after colloidal resin adsorptions. The topography and phase contrast images after colloid adsorption at low and high ionic strength are shown in Figure 5.17.

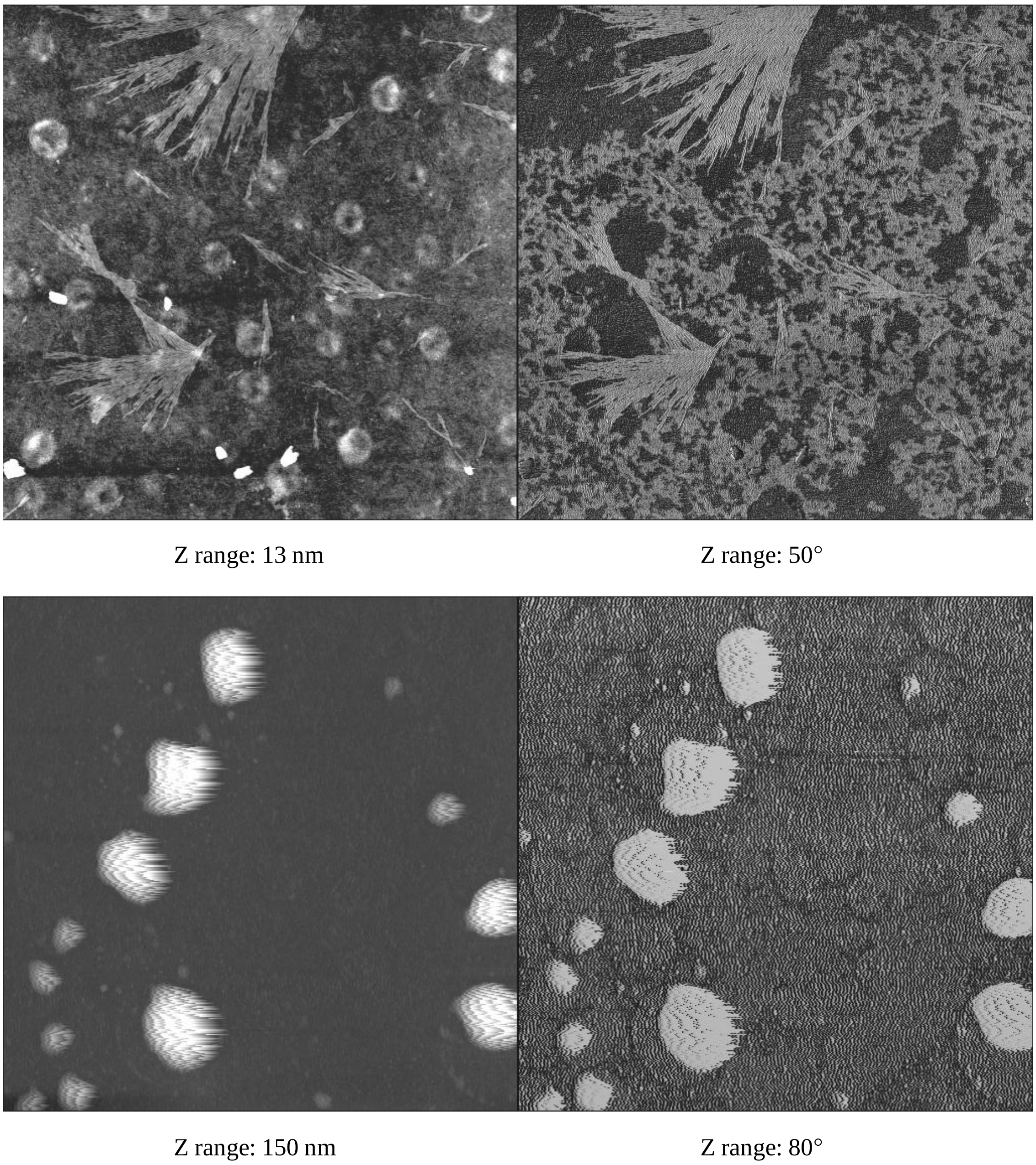

Figure 5.17. AFM topography (left) and phase contrast (right) of extractives on cellulose at low ionic strength (top) and high ionic strength (bottom). Image size is 5 μm^2. (unpublished results)

As shown in Figure 5.12, the electrostatically stable extractive colloids extensively adsorbed on cellulose surface and the adsorption increased with increasing ionic strength. AFM images indicate the spreading of colloids and the film formation on the cellulose surface. Small circle features detected in the height image at low ionic strength originate from cellulose surface. These features are often detected on pure cellulose surface when it has been kept in water. In phase contrast image the circular features are not detected which supports the conclusion that they originate from cellulose. Extractives seem to appear as a relatively thin film as light areas on cellulose surface and the film do not fully cover the cellulose surface. The scanning of the surfaces is carried out using light tapping, thus, the phase shift is the most probably due to the differences in hydrophobicity between cellulose and extractives. The extractives are interpreted as light areas in the phase contrast image since adhesion between hydrophilic tip and hydrophobic extractive film is lower than the adhesion between hydrophilic tip and hydrophilic cellulose. The similar conclusions are drawn by Österberg et al. (2005 and 2006) when thin extractive film is detected on fibre and paper surfaces.

At high ionic strength it seems that extractives fully cover the cellulose surface. This conclusion was supported by the QCM-D results when large frequency and dissipation changes were detected (Figure 5.12b). The noise when scanning such a film was relatively high due to the sticky nature of the extractives. A similar kind of interference was detected when model films of wood extractives were scanned, see Figure 5.6. The deposited extractives appeared also as colloids as seen in both topography and phase contrast images in Figure 5.17. The size of the droplets detected is within the size distribution of extractive colloids.

Similar kind of colloidal particles were not observed at the cellulose surface at low ionic strength. It seems that when the surface is fully covered with the extractive film, the additional colloids do not spread on the surface to any further extent. The QCM-D experiments showed that extractive colloids adsorbed on extractive surface only in minor amounts, if any, see Figure 5.12. Thus, the colloids do not have any specific affinity towards extractive film and they retain their colloidal shape as seen in the AFM image.

The similar kind of film formation of extractives was also detected on the paper surfaces, when paper sheets were prepared using very extractive rich white waters, see Figure 5.18 and especially the areas inside the black squares.

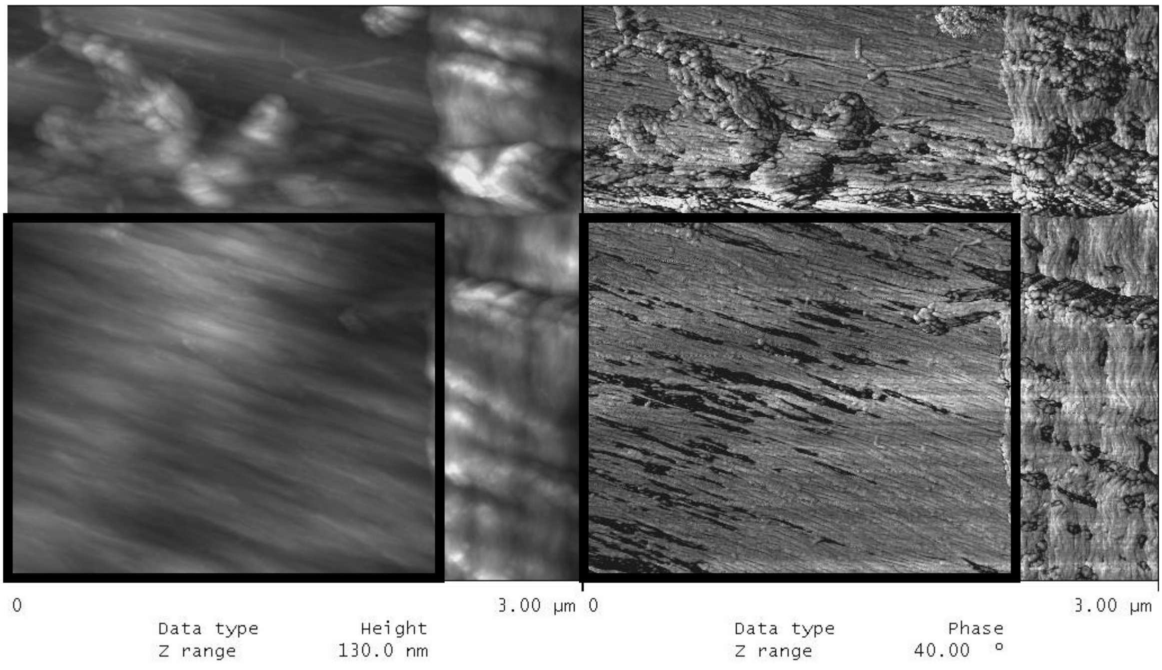

Figure 5.18. AFM topography (left) and phase contrast (right) of extractives on the MBF sheet (Moving Belt Former). Image size is 3 μm^2. The MBF sheets were provided by Lionel Clerc, Laboratory of Paper and Printing Technology, TKK. (unpublished results)

Light, film like areas seen in the phase contrast image inside the black box were identified to be extractive film spread on the paper surface. The area is very smooth (see topography image) and hence the contrast observed in the phase image is not due to topography but interpreted to be due to a thin film of extractives almost fully covering the fibre surface. It was shown that if an excessive amount of wood extractives were added to the pulp, the extractives adsorbed on the fiber surface. These results were in the scope of the other part of the project and are not further discussed here. However, the results showed that by combining more practical sheet experiments and detailed investigations of fundamental surface chemistry studies, an insight into the behavior of the dissolved and colloidal substances during papermaking could be gained.

6 CONCLUSIONS

QCM-D technique is highly suitable for to the adsorption studies using papermaking chemicals and other components such as wood polymers and extractive colloids. The dependence of the structure and viscoelastic properties of the adsorbed layer on charge density, molecular weight and electrolyte concentration does not differ from the well-known behavior of the randomly coiled linear polyelectrolyte. This was verified by using a fairly simple system of cationic starch which was adsorbed on the oppositely charged silica surface. Adsorption increased with increasing electrolyte concentration and molecular weight, and with decreasing charge density of the polyelectrolyte. Starch with narrow molecular weight distribution formed a more compact and rigid layer due to the better packing of the starch molecules when compared to the starch with broad molecular weight distribution.

The substrate surfaces prepared for the QCM-D instrument, which model the real main fiber components were developed and further characterized with AFM and XPS. Lignin, cellulose and extractive films were rigidly attached on the polystyrene coated QCM-D crystal. Cellulose and lignin films were stable and their physical properties did not significantly change when the ionic strength was changed. Some swelling but no layer softening was detected with the cellulose film in aqueous solution. In the case of lignin surface some liquid penetration but no swelling was detected and the extractive surface was stable at neutral and acidic conditions. The proper use of the model surface requires a sufficient stabilization time prior to the adsorption experiments. All the surfaces were suitable for adsorption experiments with QCM-D and repeatable results were obtained.

Dissolved hemicelluloses and colloidal extractives isolated from TMP were adsorbed on each model surface. It was found that dissolved hemicelluloses adsorbed at the largest on cellulose. They adsorbed also on extractives but towards lignin there was no significant affinity. It was shown that the hemicellulose film formed on lignin was not relatively strongly bound and probably in the presence of higher shear rates the hemicellulose film easily desorbs from the lignin surface. Adsorption increased with increasing ionic strength on cellulose and on extractives. These results show clearly why the hemicelluloses isolated from unbleached TMP can effectively sterically stabilize extractive colloids. The hemicelluloses, indeed, adsorb extensively on the extractives and also on cellulose forming a layer with loops and tails pointing out the solution phase.

Less hemicelluloses, isolated from peroxide bleached TMP, adsorbed on each surface due to the higher repulsion between charged carboxylic acid segments and smaller size of the molecules. The adsorption behavior of pure model hemicelluloses, O-acetyl-galactoglucomannan (GGM) and pectin, gave the additional evidence backing the results. Pure pectin adsorbed forming a very thin, flat and rigid layer. GGM adsorbed extensively on extractives, which indicates that galactoglucomannans play a main role when creating steric hindrance around the colloidal extractives.

Colloidal extractives adsorbed the most preferentially on cellulose when only electrostatically stabilized and the adsorption increased with increasing electrolyte concentration. If both, the colloids and the model surfaces, were sterically stabilized by hemicelluloses, the colloid adsorption was prevented. This finding explains the colloidal extractive adsorption differences on flake-type and on fibrillar fines. It was shown that sterically stabilized extractive colloids adsorb on lignin rich flakes but remain in the solution phase in the presence of fibrillar fines. Sterically stabilized colloids probably adsorb on lignin containing areas. These areas are left uncovered because the hemicelluloses do not significantly attach on lignin.

Additional knowledge of spreading of extractives on cellulose surface was also gained with AFM. It was shown that by combining practical problems and fundamental surface chemistry studies, the behavior of the dissolved and colloidal substances during papermaking can be further clarified.

REFERENCES

1. Aguié-Béghin V., Baumberger, S., Monties, B. and Douillard, R. *Langmuir* **2002**, *18*, 5190.

2. Albrecht, T.R., Grütter, P., Horne, D., Rugar, D. *J. Appl. Phys.* **1991**, *69*, 668.

3. Alen, R., Structure and chemical composition of wood. In: Stenius, P. (ed.) *Forest Products Chemistry*, Papermaking Science and Technology, Book 3, Fapet Oy, Jyväskylä, Finland 2000, 12-57.

4. Allen, L.H. Pulp. Pap. Can. **1975**, *76*, T139.

5. Ashley, J.C. and Williams, M.W. *Radiation Res.* **1980**, *81*, 364.

6. Bar, G., Thomann, Y., Brandsch, R., Cantow, H.-J and Whangbo, M.-H. *Langmuir* **1997**, *13*, 3807.

7. Barnes, H.A., Hutton, J.F. and Walters, K., *An Introduction to Rheology*, Rheology Series, 3, Elsevier, Amsterdam, 1989, pp. 199.

8. Binnig, G., Quate, C.F. and Greber, Ch. *Physical Review Letters* **1986**, *56*, 930.

9. Björkman, A. *Svensk papperstidn*. **1956**, *60*, 477.

10. Blodgett, K.B. *J. Am. Chem. Soc.* **1935**, *57*, 1007.

11. Bornside, D.E., Brown, R. A., Ackmann, P. W., Frank, J. R. F., Tryba, A. A. and Geyling, F. T. *J. Appl. Phys.* **1993**, *73*, 585.

12. Brandal, J. and Lindheim, A. *Pulp Pap. Mag. Can.* **1966**, *67*, T431.

13. Briggs, D. and Seah, M.P. (Eds.), Practical Surface Analysis, Vol. 2: *Ion and Neutral Spectroscopy*, 2 ed. Wiley, New York, 1992.

14. Brinen, J. S., greenhouse, S. and Dunlop-Jones, N. *Nordic Pulp Pap. Res. J.* **1991**, *6*, 47.

15. Böhmer, M.R., Evers, O.A., Scheutjens, J.M.H.M., *Macromolecules*, **1990**, *23*, 2288.

16. Börås, L and Gatenhol, P. *Holzforschung* **1999**, *53*, 188.

17. Börås, L and Gatenhol, P. *Holzforschung* **1999**, *53*, 429.

18. Chibowski, J., *J. Colloid Interface Sci.*, **1990**, *143*, 174.

19. Constantino, C.J.L., Juliani, L.P., Botaro, V.R., Balogh, D.T., Pereira, M.R., Ticianelli, E.A., Curvelo, A.A.S and Oliveira Jr. O.N. *Thin Solid Films* **1996**, *191*, 284.

20. Cooper G. K., Sandberg K. R. and Hinck J. F. *J. Appl. Polym. Sci.* **1981**, *26*, 3827.

21. Day, D. and Lando, J. *Macromolecules* **1980**, *13*, 1478.

22. Derjaguin, B.V. and Landau, L. *Acta Physicochimica URSS* **1941**, *14*, 633.

23. Dijt, J.C., Cohen Stuart, M.A., Fleer, G.J., *Adv. Colloid. Interf. Sci.* **1994**,*50*, 79.

24. Dorris, G. M and Gray, D., *Cellul. Chem. Technol* **1978a**, *12*, 721.

25. Dorris, G. M and Gray, D., *Cellul. Chem. Technol* **1978b**, *12*, 9.

26. Dukhin, S.S., Kretzschmar, G. and Miller, R., *Dynamics of Adsorption at liquid interfaces*, Elsevier Science B.V., The Netherlands, 1995, 581 p.

27. Eisenriegler, E., *Polymers Near Surfaces, Conformation Properties and Relation to Critical Phenomena*, World Scientific Publishing Co. Pte. Ltd., Singapore, 1993, 412 p.

28. Fardim, P., Gustafsson, J. von Schoultz, S., Peltonen, J., Holmbom, B. *Coll. Surf. A* **2005**, *225*, 91.

29. Ferry, J.H., *Viscoelastic Properties of Polymers*, 3. ed., John Wiley & Sons, New York, 1980, pp. 641.

30. Fleer, G.J., Cohen Stuart, M.A., Scheutjens, J.M.H.M. Cosgrove, T. and Vincent, B., *Polymers at Interfaces*, Chapman&Hall, University Press, Cambridge, 1993, 502 p.

31. Flory, P.J., *Principles of Polymer Chemistry*, Cornell University Press: Ithaca, NY, 1953.

32. García, R and Pérez, R. *Surf. Sci. Reports* **2002**, *47*, 197.

33. Granfeldt, M.K., Jönsson, B., Woodward, C.E., *J. Phys. Chem.* **1992**, *96*, 10080.

34. Greber G. and Paschinger O. *Das Papier* **1981** *35*, 547.

35. Gray, D. *Cellulose Chem. Technol.* **1978**, *12*, 735.

36. Gustafsson, J., Lehto, J. H., Tienvieri, T., Ciovica, L and Peltonen, J. *Colloids Surf. A: Physicochem. Eng. Aspects* **2003**, *225*, 95.

37. Hamaker, C.H. *Physica* **1937**, *4*, 1058.

38. Hanley, S. J., Giasson, J., Revol, J.-F. and Gray, D. *Polymer* **1992**, *33*, 4639.

39. Hanley, S.J. and Gray, D. *Holzforschung* **1994**, *48*, 29.

40. Hannuksela, T., Tenkanen, M. and Holmbom, B. *Cellulose* **2002**, *9*, 251.

41. Hannuksela, T. and Holmbom, B. Sorption of mannans onto different fiber surfaces – an evolution of understanding. In: Hemicelluloses: Science and Technology, Gatenholm, P. and Tenkanen, M. (eds), ACS symposium series 864, 2003a, 222-235.

42. Hannuksela, T., Fardim, P. and Holmbom, B. *Cellulose* **2003b**, *10*, 317.

43. Hannuksela, T. and Holmbom, B. *J Pulp Pap. Sci.* **2004a**, *30*,159.

44. Hannuksela, T., Holmbom, B., Mortha, G. and Lachenal, D. *Nord. Pulp Pap. Res. J.* **2004b**, *19*, 237.

45. Holmberg, M., Berg, J., Stemme, S., Ödberg, L., Rasmusson, J. and Claesson, P. *J. Colloid Interface Sci.* **1997**, *186*, 369.

46. Holmbom, B., Ekman, R., Sjöholm, R., Eckerman, C. and Thorton, J. *Papier* **1991**, *45*, V16.

47. Holmbom, B. and Sundberg, A. *Wochenblatt für papierfabrikation* **2003**, *21*, 1305.

48. Höök, F., Rodahl, M., Brzezinski, P., Kasemo, B., *Langmuir*, **1998**, *14*, 7290.

49. Israelachvili, J. *Intermolecular & Surface Forces*, 2. ed., Academic Press Limited, London, 1992, pp. 450.

50. Johansson, L-S., Campbell, J.M., Koljonen, K. and Stenius, P., *Appl. Surf. Sci.* **1999**, 144-145, 92.

51. Johansson, L-S., *Microchimica Acta* **2002**, *138*, 217.

52. Johansson, L.-S., Campbell, J.M. Fardim, P., Hultén, A. H., Boisvert, J.-P. and Ernstsson, M. *Surface Science* **2005**, *584*, 126.

53. Johnsen, I. A., Lenes, M. and Magnusson, L**.** *Nord. Pulp Paper Res. J.* **2004**, *19*, 22.

54. Jönsson, B., Lindman, B., Holmberg, K. and Kronberg, B., *Surfactants and Polymers in Aqueous solution.* John Wiley & Sons Ltd, England, 1998, 438 p.

55. Kangas, H and Kleen, M. *Nordic Pulp Paper Res. J.* **2004**, *19*, 191.

56. Kleen, M., Kangas, H. and Laine, C. *Nordic Pulp Paper Res. J.* **2003**, *18*, 361.

57. Koljonen, K., Österberg, M., Johansson, L.-S. and Stenius, P. *Colloids Surfaces A: Physicochem. Eng. Aspects.* **2003**, *228*, 143.

58. Koljonen, K., Österberg, M., Kleen M., Fuhrmann, A. and Stenius, P. *Cellulose* **2004**, *11*, 209.

59. Kolthoff, J.M. and Gutmacher, J., *J. Phys. Chem.*, **1952,** *56*, 740

60. Kokkonen, P., Korpela, A., Sundberg, A and Holmbom, B. *Nordic Pulp Paper Res. J.* **2002**, *17*, 382.

61. Kokkonen, P., Fardim, P. and Holmbom, B. *Nordic Pulp Paper Res. J.* **2004**, *19*, 318.

62. Kontturi, E., Tammelin, T. and Österberg, M. Chemical Society Reviews, 2006, DOI:10.1039/B601872F

63. Langmuir, I. *J. Am. Chem. Soc.* **1917**, *39*, 1848.

64. Langmuir, I. and Schaefer, V.J. *J. Am. Chem. Soc.* **1938**, *60*, 1351.

65. Lee, S., Virtanen, J.A., Virtanen, S.A. and Penner, R. M. *Langmuir* **1992**, *8*, 1243.

66. Lifshitz, E.M. *Soviet Phys. JETP (Eng Transl.)* **1956**, *2*, 73.

67. Lindholm, C.-A., Bleaching In: Sundholm, J. (ed.) *Mechanical Pulping*, Papermaking Science and Technology, Book 5, Fapet Oy, Jyväskylä, Finland 1999, 313-343.

68. Liu, G., Guillet, J.E., Al-Takrity, E.T.B., Jenkins, A.D., Walton, D.R.M., *Macromolecules*, **1991**, *24*, 68.

69. Luukko, K and Paulapuro, H. *Tappi J.* **1999**, *82*, 95.

70. Luukko, K., Laine, J. and Pere, J. *Appita J.* **1999**, *52*, 126.

71. Magonov, S.N. and Whangbo, M.-H. *Surface Analysis with STM and AFM*, Wiley-VCH, Weinheim, 1996.

72. Martin, Y., Williams, C.C., Wickramasinghe, H.K. *J. Appl. Phys.* **1987**, *61*, 4723.

73. Marton, J. and Marton, T., *Tappi*, **1976,** *59*, 121.

74. Meyerhofer, D. *J. Appl. Phys.* **1978**, *49*, 3993.

75. Mosbye, J., Moe, S. and Laine, J. *Nord. Pulp Paper Res. J.* **2002**, *17*, 352.

76. Mosbye, J., Laine, J. and Moe, S. *Nordic Pulp Paper Res. J.* **2003**, *18*, 63.

77. Niemi, H., Paulapuro, H. and Mahlberg, R. Paper and Timber **2002**, *84*, 389.

78. Norgren, M., Notley, S. M., Majtnerova, A and Gellerstedt, G. *Langmuir* **2006**, *22*, 1209.

79. Odijk, T., *J. Polym. Sci. Polym. Phys. Ed.*, **1978**, *16*, 627.

80. Oliveira Jr. O.N., Constantino, C.J.L., Balogh, D.T., and Curvelo, A.A.S. *Cell. Chem. Technol.* **1994**, *28*, 541.

81. Otero, D., Sundberg, K., Blanco, A., Negro, C., Tijero, J. and Holmbom, B. *Nord. Pulp Pap. Res. J.* **2000**, *15*, 607.

82. Pasquini, D., Balogh, D.T., Oliveira Jr., O.N. and Curvelo, A.A.S. *Colloids Surf. A: Physicochem. Eng. Aspects* **2005,** *252*, 193.

83. Petty, M. C. *Langmuir-Blodgett films, An introduction.* Cambridge University Press, Cambridge 1999.

84. Pirttinen, E., Stenius, P., Vuorinen, T., Kovasin, K. and Ala-Kaila, K. TAPPI Fall Technical conference, Marriott Marquis, Atlanta, GA, October 31-November 3, 2004.

85. Plunkett, M. A., Claesson, P, M., Ernstsson, M. and Rutland, M. W. Langmuir **2003**, *19*, 4673.

86. Q-Sense D300 User Manual, Q-Sense AB 2000.

87. Roberts, G. *Langmuir-Blodgett Films*. Plenum Press, New York, 1990.

88. Roberts, J.C., *The chemistry of paper*, The royal society of chemistry, UK, 1996, 190 p.

89. Rodahl, K., Höök, F., Krozer, A., Brezezinski, P., Kasemo, B., *Rev. Sci. Instrum.*, **1995**, *66*, 3924.

90. Schaub M., Wenz G., Wegner G., Stein A. and Klemm D. *Adv. Mater.* **1993**, *5*, 919.

91. Scheutjens, J.M.H.M., Fleer, G.J., *J. Phys. Chem.*, **1979**, *83*,1619.

92. Scheutjens, J.M.H.M., Fleer, G.J., *J. Phys. Chem.*, **1980**, *84*,178.

93. Sihvonen, A.-L., Sundberg, K., Sundberg, A. and Holmbom, B. *Nordic Pulp Paper Res. J.* **1998**, *13*, 64.

94. Spatz, J. P., Sheiko, S., Möller, M., Winkler, R. G., Reineker, P. and Marti, O. *Langmuir* **1997**, *13*, 4699.

95. van de Steeg, H.G.G., de Keizer, A., Cohen Stuart, M.A. and Bijsterbosch, B.H., *Colloids Surfaces A: Physicochem. Eng. Aspects*, **1993**, *70*, 77.

96. Stenius, P., Palonen, H., Ström, G. and Ödberg, L. Micelle formation and phase equilibria of surface active components of wood In: *Surfactants in solution*, Mittal, K. and Lindman, B., (Editors), Plenum Publishing Co, New York, Vol. 1, 1984, 153-174.

97. Stenius, P., Macromolecular, surface and colloid chemistry. In: Stenius P. (ed.) *Forest Products Chemistry*, Papermaking Science and Technology, Book 3, Fapet Oy, Jyväskylä, Finland, 2000, 172-276.

98. Ström, G. (2000): Physico-chemical properties and surfactant behavior. In: *Pitch control, wood resin and deresination*, Back, E.L., Allen, L.H. (Editors), Tappi Press, Atlanta, GA, pp. 139-149, and references therein.

99. Sukanek, P.C. *J. Electrochem. Soc*. **1991**, *138*, 1712, and references therein.

100. Sundholm, J., What is mechanical pulping? In: Sundholm, J. (ed.) *Mechanical Pulping*, Papermaking Science and Technology, Book 5, Fapet Oy, Jyväskylä, Finland 1999, 17-21.

101. Sundberg, A., Sundberg, K., Lillandt, C. and Holmbom, B. *Nord. Pulp Paper Res. J.* **1996a**, *8*, 216.

102. Sundberg A,. Holmbom, B., Willför, S. and Pranovich, A., *Nord. Pulp Pap. Res. J.* **2000**, *15*, 46.

103. Sundberg, K., Thorton, J., Ekman, R. and Holmbom, B. *Nord. Pulp Pap. Res. J.* **1994a**, *9*, 125.

104. Sundberg, K., Thorton, J., Petterson, C., Holmbom, B and Ekman, R. *J. Pulp Pap. Sci.* **1994b**, *20*, J317.

105. Sundberg, K., Petterson, C., Eckerman, C. and Holmbom, B. *J. Pulp Paper Sci.* **1996b**, *22*, 248.

106. Sundberg, K., Thorton, J., Holmbom, B and Ekman, R. J. Pulp Pap. Sci. **1996c** *22*, J226.

107. Tammelin, T., Österberg, M. and Laine, J., Viscoelastic properties of the adsorbed hemicellulose layers, Manuscript, 2006.

108. Thorton, J., Ekman, R., Holmbom, B. and Örså, F. *J. Wood Chem. Technol.* **1994**, *14*, 159.

109. Verwey, E.J.W. and Overbeek, J. Th. G. *Theory of Stability of Lyophobic Colloids*, Elsevier, Amsterdam, 1948.

110. Voinova, M., Rodahl, M., Jonson, M., Kasemo, B., *Phys. Scr.* **1999** *59*, 391.

111. Willför, S., Rehn, P., Sundberg, A., Sundberg, K. and Holmbom, B. *Tappi J.* **2003**, *2*, 27.

112. Wågberg, L. and Ödberg, L., *Nordic Pulp Paper Res. J.*, **1989**, *2*, 135.

113. Wågberg, L and Annergren, G. 1997, Physicochemical characterization of papermaking fibres. In: Baker, C.F. (ed) *The fundamentals of papermaking materials*: Transactions of the 11th Fundamental research Symposium, Cambridge, England. Leatherhead, Pira International, pp. 1-82.

114. Zhong, Q., Imniss, D., Kjoller, K., Elings, V.B. *Surf. Sci.* **1993**, *290*, L688.

115. Örså F. and Holmbom, B. *J. Pulp Paper Sci.* **1996**, *20*, 361.

116. Österberg, M., Koljonen, K. and Johansson, L.-S., Proceedings of the 13th International Symposium on Wood, Fibre and Pulping Chemistry, Vol 2, Appita, Victoria, Australia, 2005, 69.

117. Österberg, M., Schmidt, U., Jääskeläinen, A.-S. Colloids Surf. A: Physicochem. Eng. Aspects 2006, DOI:10.1016/j.colsurfa.2006.06.039.